Fundamental properties of ZnO nanostructures

 DOI: 10.1002/cphc.200700002 © 2007 Wiley-VCH Verlag GmbH & Co. KGaA, Weinheim

DOI: 10.1002/cphc.200700002

ZnO: Material, Physics and Applications

C. Klingshirn*[a]

ZnO is presently experiencing a research boom with more than 2000 ZnO-related publications in 2005. This phenomenon is triggered, for example, by hope to use ZnO as a material for blue/UV optoelectronics as an alternative to GaN, as a cheap, transparent, conducting oxide, as a material for electronic circuits that are transparent in the visible or for semiconductor spintronics. Currently, however, the main problem is to achieve high, reproducible and stable p-doping. Herein, we critically review aspects of the material growth, fundamental properties of ZnO and ZnO-based nanostructures and doping as well as present and future applications with emphasis on the electronic and optical properties including stimulated emission.

1. Introduction

Zincoxide is a II^b–VI compound semiconductor. The II^b–VI semiconductors and semimetals comprise the binary compounds of Zn, Cd, and Hg with O, S, Se, and Te and their ternary or quaternary alloys. ZnO is a wide-gap semiconductor with a direct gap around 3.4 eV (i.e. in the near-UV) and crystallises preferentially in the hexagonal wurtzite-type structure. It occurs in nature with the mineral name zincite. The mineral usually contains a certain amount of manganese and other elements and is of yellow to red colour. The ZnO used for the investigations and applications described below is exclusively synthetic material. Due to its large band gap, pure ZnO is colourless and clear.

Research on ZnO started gradually in the 1930s. This early period is reviewed and documented, for example, in refs. [1–3]. The research peaked around the end of the seventies and the beginning of the eighties. Then the interest faded, partly because it was not possible to dope ZnO in both an n- and p-type manner, which is an indispensable prerequisite for applications of ZnO in optoelectronics, and partly because the interest shifted to structures of reduced dimensionality, like quantum wells, which were at that time almost exclusively based on the III–V system $GaAs/Al_{1-y}Ga_yAs$. The emphasis of ZnO research at that time was essentially on bulk samples covering topics like growth, doping, transport, deep centres, band structure, excitons, bulk and surface polaritons, luminescence, high excitation or many-particle effects and lasing. Results of this first research period are reviewed, for example, in refs. [4–8] and entered in data collections[9] or in textbooks on semiconductor optics.[10]

The present renaissance in ZnO research started in the mid 1990s and is documented by numerous conferences, workshops, and symposia and by more than 2000 ZnO-related papers in the year 2005 and even higher numbers in 2006, compared to slightly beyond 100 in 1970 (sources: INSPEC, Web of Science).

The considerable current interest is based on the possibility to grow epitaxial layers, quantum wells, nanorods and related objects or quantum dots and on the hope to obtain:

- a material for blue/UV optoelectronics, including light-emitting or even laser diodes in addition to (or instead of) the GaN-based structures
- a radiation hard material for electronic devices in a corresponding environment
- a material for electronic circuits, which is transparent in the visible
- a diluted or ferromagnetic material, when doped with Co, Mn, Fe, V or similar elements, for semiconductor spintronics
- a transparent, highly conducting oxide (TCO), when doped with Al, Ga, In or similar elements, as a cheaper alternative to indium tin oxide (ITO).

For several of the above-mentioned applications, a stable, high, and reproducible p-doping is obligatory. Though progress has been made in this crucial field, as will be outlined below, this aspect still represents a major problem.

The emphasis of present ZnO research is essentially on the same topics as earlier, but it also includes nanostructures, new growth and doping techniques, and it focuses more on application-related aspects. For first reviews of this new ZnO research period, see, for example, refs. [11–16]. In the following, we shall deliberately present or cite both old and new results covering six decades of ZnO research.

We will consider growth and some of the fundamental properties of bulk ZnO and of nanostructures and structures of reduced dimensionality with emphasis on (partly critical) reviewing of the electronic and optical properties. The next larger section is devoted to high excitation effects, stimulated emission and lasing, again covering the range from bulk material over quantum wells and nanorods to quantum dots. In the last section, we treat past, present and possible future applications of ZnO. We also give short introductions to the various concepts of semiconductor optics, which may not be so familiar to

[a] *Prof. Dr. C. Klingshirn*
Institut für Angewandte Physik der Universität Karlsruhe
Wolfgang-Gaede-Str. 1, 76131 Karlsruhe (Germany)
Fax: (+49) 721-608-3410
E-mail: Claus.Klingshirn@physik.uni-karlsruhe.de

 © 2007 Wiley-VCH Verlag GmbH & Co. KGaA, Weinheim WILEY InterScience DISCOVER SOMETHING GREAT

the readership. For details we recommend, for example, ref. [10].

2. Crystal Structure and Chemical Binding[1]

Zinc oxide crystallises in the hexagonal wurtzite-type structure shown in Figure 1. It has a polar hexagonal axis, the ***c*** axis, chosen to be parallel to *z*. The point group is in the various notations 6 mm or C_{6v}, the space group $P6_3mc$ or C_{6v}^4. One zinc ion is surrounded tetrahedrally by four oxygen ions and vice versa. The primitive unit cell contains two formula units of ZnO. The ratio c/a of the elementary translation vectors, with values around 1.60, deviates slightly from the ideal value $c/a=\sqrt{8/3}=1.633$.[9] In contrast to other II^b–VI semiconductors, which exist both in the cubic zinc blende and the hexagonal wurtzite-type structures (like ZnS, which gave the name to both structures), ZnO crystallises with great preference in the wurtzite-type structure. The cubic zinc blende-type structure can, to some extent, be stabilised by epitaxial growth of ZnO on suitable cubic substrates, while the rock salt structure is stable only under pressure.[17]

Figure 1. Unit cell of the crystal structure of ZnO . The light grey spheres corresponds to oxygen, the dark ones to zinc. The primitive translation vectors ***a*** and ***b*** include an angle of 120° and are situated in the base plane, ***c*** is orthogonal to them (from Wikipedia)

The tetrahedrally coordinated diamond, zinc blende, and wurtzite-type crystal structures are characteristic for covalent chemical binding with sp^3 hybridisation. While the Group IV element semiconductors like diamond, silicon and germanium have completely covalent bonding, one has an increasing admixture of ionic binding when going from the Group IV over the III–V and II^b–VII to the I^b–VII semiconductors, ending with completely ionic binding for the II^a–VI and I^a–VII insulators like MgO or NaCl, which frequently crystallise in the rock salt structure.[10]

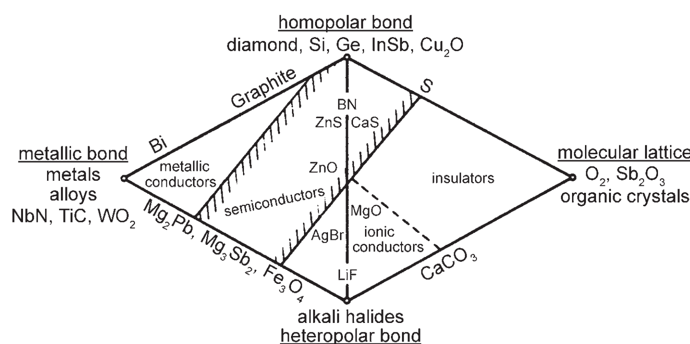

Figure 2. Schematic drawing of various types of chemical bonding of solids and their electronic properties.[18]

ZnO already has a substantial ionic bonding component, as shown in the "historic" diagram of Figure 2, which shows ZnO in the "centre of solid state physics".

Because of this fraction of ionic binding, the bottom of the conduction band, or the lowest unoccupied orbital (LUMO), is formed essentially from the 4s levels of Zn^{2+} and the top of the valence band, or highest occupied molecular orbital (HOMO), from the 2p levels of O^{2-}. The band gap between the conduction and valence bands is about 3.437 eV at low temperatures.

3. Phonons and other Lattice Properties

Phonons are the quanta of the lattice vibrations. Due to its $s=4$ atoms per unit cell, ZnO has three acoustic phonon bands, two transverse and one longitudinal as in every solid, and $(3s-3)=9$ optical ones.

The eigenenergies of the optical phonons with momentum $\mathbf{k}=0$, that is, at the Γ-point, the centre of the first Brillouin zone, range from 12.3 to 72.5 meV.[9] The Γ_1 and Γ_5 states are optically dipole-allowed for the polarisations $\boldsymbol{E}\parallel\boldsymbol{c}$ and $\boldsymbol{E}\perp\boldsymbol{c}$, respectively, where ***c*** is the polar hexagonal axis and ***E*** the electric field. The optical Γ_1 and Γ_5 phonons lead in the IR to distinct stop (or Reststrahl) bands for $\boldsymbol{E}\parallel\boldsymbol{c}$ and $\boldsymbol{E}\perp\boldsymbol{c}$, with transverse and longitudinal eigenfrequencies around 50 and 72 meV. The Γ_1, Γ_5, Γ_6 modes are also observed in Raman scattering.[9,15] The fact that some phonon modes are seen both in the IR spectra as stop bands and in Raman spectra is due to

[1] *Pictures of the hexagonal unit cell of the wurtzite structure are given in various reviews, for example, refs. [2,11,16]. It should be noted that both the zinc blende and the rocksalt structure are face-centred cubic (fcc) structures and therefore have the same primitive unit cell. They differ only by the arrangement of the atoms within one unit cell, the so-called basis. The unit cells shown in Figure 1.2 of ref. [16] for the zinc blende-type modification of ZnO is not primitive, and the one for rock salt is not a unit cell at all.*

Claus F. Klinghirn earned both his Diplom (1971) and Ph.D. (1975) degrees at the University of Erlangen under the supervision of Prof. Dr. E. Mallwo, one of the pioneers of ZnO research. After his habilitation at the University of Karlsruhe in 1980, he became an associate professor at the University of Frankfurt am Main before he received and accepted offers for a chair/full professorship at the universities of Kaiserslautern and Karlsruhe in 1987 and 1993, respectively. His fields of research include the (non)linear, temporally or spatially resolved spectroscopy of semiconductors and their growth by molecular beam epitaxy. He has authored or co-authored more than 400 publications in refereed journals, as book chapters, or in conference proceedings. He is co-editor of various volumes of the data collection Landolt-Börnstein and of the RÖMPP Lexicon Chemie and author of the textbook Semiconductor Optics, which just appeared in its third edition.

 © 2007 Wiley-VCH Verlag GmbH & Co. KGaA, Weinheim

the fact that the wurtzite structure does not have a centre of inversion, that is, the parity of the wave functions is not a good quantum number.[10,19,20]

For recent data on isotopically pure ZnO, where phonons no longer show inhomogeneous broadening due to the different isotope masses, see ref. [20].

The fact that ZnO has (partial) ionic bonding and lacks a centre of inversion is also the origin of the piezoelectricity of ZnO. The three coefficients of the piezoelectric tensor, d_{15}, d_{31} and d_{33}, are rather large, with values around -10, -5 and $12\times 10^{-12}\,\mathrm{m\,V^{-1}}$, respectively.[9,15,21]

For elastic coefficients of ZnO, its hardness and its thermal properties, such as specific heat, Debye temperature or thermal conductivity, see ref. [9] and references therein.

4. Growth

Bulk ZnO samples are grown by various techniques. A possibility to grow ZnO by gas transport is given by the following reactions

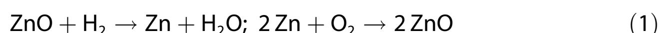

$$ZnO + H_2 \rightarrow Zn + H_2O;\; 2\,Zn + O_2 \rightarrow 2\,ZnO \tag{1}$$

Alternatively, one can start directly from Zn vapour, and sometimes graphite is used instead of H_2 for the reduction of Zn.

Pressed or sintered samples of high-purity ZnO powder are reduced to Zn vapour at elevated temperatures by hydrogen (or the addition of graphite) and transported with a flow of inert gas, such as N_2. The zinc vapour is then oxidised in a region of lower temperature under the admission of oxygen or air. Platelets and especially beautiful hexagonal needles can be grown with diameters up to several millimetres and length of several centimetres. See, for example, Figure 3a. During this process crystals sometimes develop not a pointed top but umbrella-like shape with a plane $\perp \boldsymbol{c}$. If this process occurs repeatedly "Christmas tree" structures like that shown in Figure 3c may evolve.

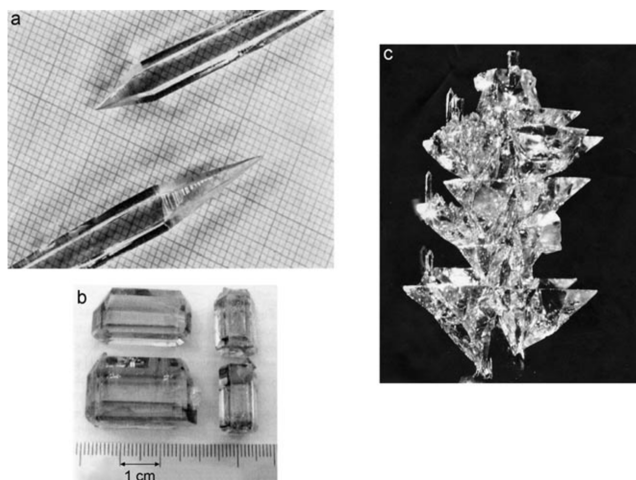

Figure 3. ZnO single crystals grown by gas transport (a, c)[23] and by hydrothermal growth (b).[25]

Some selected references for gas transport techniques are given in refs. [3,22,23].

The hydrothermal technique results in samples with volumes of many cubic centimetres (Figure 3b) and allows the production of wafers of several square centimetres for homo- or heteroepitaxy.[24,25] In this case, ZnO is dissolved at high temperatures and pressure in KOH/LiOH base in an autoclave and is precipitated at regions of reduced temperature. Other techniques include growth from melt or flux.[26] These techniques can also allow the growth of large samples.

There are also a variety of methods available for the production of textured or epitaxial layers and thin films, including quantum wells. For early examples of ZnO epitaxy, see refs. [27–29]. A relatively simple technique is to evaporate a thin and homogeneous layer of Zn, for example, on a plate of quartz glass and to subsequently oxidise it at elevated temperatures.[28] This procedure results in textured ZnO layers with the $\boldsymbol{c}$-axis normal to the substrate. The optical properties of such layers tend to be almost identical over more than six decades.[28,30] Another simple possibility is close-distance evaporation of ZnO on saphire (Al_2O_3) substrates with various orientations.[29]

The substrates suitable for epitaxy of ZnO include Al_2O_3, partly with a GaN buffer; the latter also has a wurtzite structure and only a small lattice mismatch of 1.8% to ZnO. There has been a large choice of other substrates that have been used for epitaxial ZnO growth, such as Zn, SiO_2, AlN, SiC, Si and GaAs, or more exotic ones, such as $ScAlMgO_4$, $LiTaO_3$ and $LiNbO_3$,[19] and, of course, ZnO for homoepitaxy. From the large number of relevant papers, we can give only a tiny selection in ref. [31]. See also refs. [12,14–16].

The main epitaxial methods currently used to grow epilayers or even quantum wells (either ZnO wells with $Mg_{1-y}Zn_yO$ barriers or $Zn_{1-y}Cd_yO$ wells between ZnO barriers) are partly the standard ones, such as molecular beam epitaxy (MBE), metal–organic chemical vapour deposition/metal–organic vapour phase epitaxy (MOCVP/MOVPE) using the decomposition and subsequent ZnO formation of zinc compounds such as dimethylzinc or diethylzinc with an oxygen source such as O_2, H_2O_2, H_2O, N_2O, NO_2, isopropyl alcohol, *tert*-butonyl alcohol or acetone on a heated substrate. It should be noted that MgO and CdO crystallise in the NaCl structure. Consequently, the incorporation of larger molar fractions of magnesium and especially of cadmium in $Zn_{1-y}Mg_yO$ or $Zn_{1-y}Cd_yO$ reduces the sample quality.[31,32]

A technique that is widely used for the production of high-critical-temperature (T_c) superconductors is now also frequently used to produce ZnO films, namely pulsed laser deposition (PLD).[14,15,32] In this technique, pulsed nanosecond or picosecond lasers generally emitting in the near-UV, such as excimer or frequency-tripled NdYAG lasers, are focussed tightly on a pressed or sintered ZnO target, thus producing a plume of evaporating source material, which is deposited on a heated substrate. The plume is emitted normal to the target surface, independent of the angle of incidence of the laser beam; the angle of aperture of the plume gets narrower with increasing laser pulse energy. The high kinetic energy of the evaporating

 © 2007 Wiley-VCH Verlag GmbH & Co. KGaA, Weinheim

species results in a high surface mobility on the substrate. A low background pressure of O_2 in the recipient or a post-growth annealing in an O_2 atmosphere helps to improve the stoichiometry of the ZnO layers.

The layers grown by the various techniques mentioned above are not necessarily smooth and perfect epilayers. Often, one obtains grains or columnar structures with small hexagonal pyramids on the surface, with surface roughness from a few nanometres to a few tens of nanometres. Furthermore, layers and bulk samples may contain strain. Consequently, the full-width-at-half-maximum (FWHM) of X-ray rocking curves is often in the range from tens of arc seconds to fractions of a degree, values that are considerably larger than the those found for high-quality single crystals, which go down to almost resolution-limited values of $0.0025^\circ = 8.7''$, as shown in Figure 4.

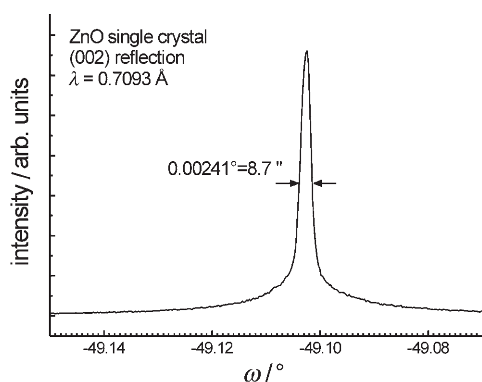

Figure 4. X-ray diffraction (ω-scan) of a ZnO crystal measured at ANKA Karlsruhe. Its growth is described in ref. [23]. From ref. [33].

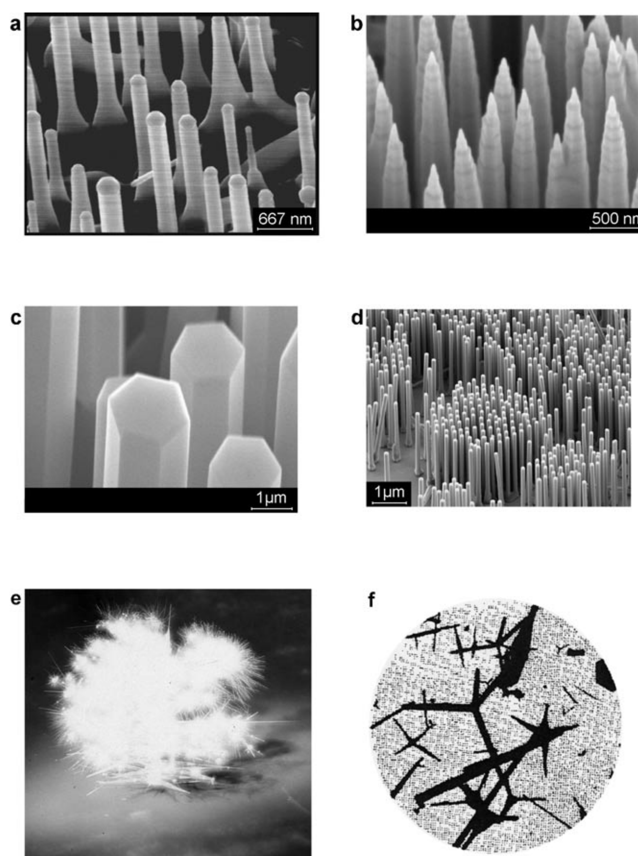

Figure 5. a)–d) A few examples of ZnO nanorods, some of which were grown by the VLS process and show the Au droplet on top (a). See the work by A. Sauer and K. Thonke (a, c), by M. Grundmann (b) in [35, 37] and M. Wissinger in [36] (d). e) A puffball of ZnO nanorods occasionally occurrs during growth.[23] f) An early example of ZnO tetrapods from 1944, at that time called fourlings, by M. L. Fuller in ref. [38].

Methods to produce large-area polycrystalline layers include radio-frequency (rf) sputtering, for example, for application of ZnO:Al as a transparent conducting oxide, spray pyrolysis or sol-gel techniques.[34]

ZnO has a strong tendency for self-organised growth. As a consequence, a very hot topic is presently the growth of whisker-like ZnO nanorods.[35] These are needle-like crystals with diameters in the range of a few tens to a few hundred nanometres and lengths of several micrometres. In Figures 5 a–d, we give a few recent examples of such structures, and in Figure 5 e an older one. The methods used to grow such nanorods include those mentioned above, such as PLD, MBE or MOCVD. A special growth procedure is the so-called vapour–liquid–solid (VLS) process. In this process, small metal clusters (usually gold) of a few tens of nanometres in diameter are deposited on a substrate. The substrate with the Au dots is heated so that the Au melts and forms a droplet. If Zn vapour is offered, Zn forms an alloy with the Au. If this alloy is supersaturated, ZnO nanorods start to grow in the presence of oxygen at the positions of the Au droplets. The Au droplets act as a catalyst and sit on top of the growing nanorods. Growth continues as long as zinc and oxygen are available and the temperature of the alloy stays above the eutectic temperature of the alloy (in Figure 5 a, the round Au droplets can be seen on top of the ZnO rods). The diameter of the growing nanorods is given by the diameter of the Au droplet. The orientation of the needles in the plane is given by the substrate, with ***c*** perpendicular to the length of the needles. In the meantime, scientists were successful in growing nanorods without the Au droplet catalyst and in growing them on non-crystalline substrates such as glass or plastic sheets. Recently, it has even become possible to grow single quantum wells or superlattices ($ZnO/Zn_{1-y}Mg_yO$) into such nanorods.[35] Apart from the "simple" nanorods shown in Figure 5, under suitable conditions ZnO also likes to grow as a variety of different nanostructures, including tetrapods, combs, brushes, nails, tubes, walls, flowers, corals, castles or propellers.[35] One or two decades ago, some of the ZnO layers of the various nanostructures would have been considered unsuccessful attempts to produce a good epitaxial layer and would have ended up in the dustbin.

It should be acknowledged that the growth of ZnO tetrapods or whiskers is not new, but goes back more than six decades, as shown in Figure 5 f from 1944.

To reduce the quasidimensionality of ZnO nanostructures even further, it has been tried successfully to grow quasi zero-dimensional ZnO quantum dots (QDs), also known as nano-

 © 2007 Wiley-VCH Verlag GmbH & Co. KGaA, Weinheim

crystals, quantum boxes, nanoislands or artificial atoms.[10] These are crystallites with typical dimensions of a few nanometres in all three directions of space, surrounded by a material with a higher band gap or by air.

The techniques for the production of such ZnO QDs are again manifold and include spray pyrolysis, the precipitation of ZnO from aquous solutions or in glasses during an annealing process, self-assembly in a Stranski–Krastanov or Volmer–Weber epitaxial growth mode or hydrolysis of $Zn(CH_300)_2$ in methanol.[39] In Figure 6, we give as an example a high-resolution transmission electron microscope (HRTEM) image of ZnO QDs grown by spray combustion of Zn/Si precursors. The lattice planes of the ZnO crystallites are clearly visible. They are surrounded by an amorphous silicate matrix.

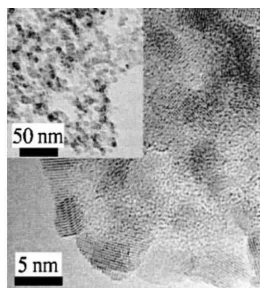

Figure 6. A high-resolution transmission electron micrograph (HRTEM) of ZnO nanocrystals.[40]

5. Electronic Band Structure

The band structure gives the electronic one-particle (i.e. electron or hole) states. Since ZnO is a direct-gap semiconductor with the global extrema of the uppermost valence and the lowest conduction bands (VB and CB, respectively) at the same point in the Brillouin zone, namely at $\mathbf{k}=0$, (i.e. at the Γ-point), we are mainly interested in this region. The lowest CB (LUMO) is formed, as already mentioned, from the empty 4s states of Zn^{2+} or the antibonding sp^3 hybrid states. The group-theoretical compatibility tables (see e.g. ref. [10] and references therein) tell us that the bottom of the CB has Γ_1 symmetry without inclusion of spin and symmetry $\Gamma_1 \otimes \Gamma_7 = \Gamma_7$ with spin (Figure 7). The effective electron (more precisely polaron) mass is almost isotropic, with a value around $m_e = (0.28 \pm 0.02) \cdot m_o$.[9]

The VB (HOMO), originating from the occupied 2p orbitals of O^{2-} or from the bonding sp^3 orbitals, is split without spin under the influence of the hexagonal crystal field into two states, Γ_5 and Γ_1. Inclusion of spin gives a further splitting (owing to spin–orbit coupling) into three twofold-degenerate sub-VBs of symmetries $(\Gamma_1 \oplus \Gamma_5) \otimes \Gamma_7 = \Gamma_7 \oplus \Gamma_9 \oplus \Gamma_7$, see Figure 7. In all wurtzite-type semiconductors (such as ZnS, CdS, CdSe, or GaN), these VBs are labelled from highest to lowest energies as A, B and C bands. In most cases, the ordering of the bands is A Γ_9 , B Γ_7, C Γ_7 and the spin–orbit splitting is larger than the crystal field splitting. In ZnO, however, there is a long standing debate over whether the ordering of the VBs is the usual one,[41] or if it is A Γ_7, B Γ_9, C Γ_7, called "negative spin–orbit splitting" or inverted VB ordering.[42] Actually, the spin–orbit splitting is always positive. But due to the small nuclear charge of oxygen, an extrapolation of the data from the II^b sulphides, selenides and tellurides to the oxides leads us to expect that this splitting is only around 10 meV. The level repulsion with the close-lying occupied Zn 4d levels may shift one Γ_7 level above the Γ_9 state, resulting in the inverted VB ordering, which is also well-established for the I^b–VII semiconductor CuCl.[43] Since the splitting of the A and B valence bands is only of the order of 5 meV, and since the selection rules are essentially the same (the transitions from the two upper A Γ_9 and B Γ_7 VBs to the Γ_7 CB band are dipole and spinflip allowed only for $\boldsymbol{E} \perp \boldsymbol{c}$, and transitions from the C Γ_7 VB are allowed only for $\boldsymbol{E} \parallel \boldsymbol{c}$), as shown in Figure 7, the discussion about the symmetries of the A and B valence bands seems to be a storm in a teacup. But frequently, such problems tend to have an extremely long decay time. As detailed in various references,[12,44] the arguments put forward recently in favour of the normal valence-band ordering in ZnO are not convincing. Therefore, we use in the following the inverted ordering: A Γ_7 , B Γ_9, C Γ_7.

The effective hole masses in ZnO are rather isotropic and similar for the A, B, and C VBs, with typical values of $m_{h\perp,\parallel A,B} = 0.59 m_0$, $m_{h\parallel C} = 0.31\, m_0$, and $m_{h\perp C} = 0.55 m_0$.[9] Bands of symmetry Γ_7 may have a small $\mathbf{k}$-linear term for $\mathbf{k} \perp \boldsymbol{c}$ as indicated in Figure 7 for the A VB. This term can also occur for the C VB (not shown here). For the CB, this effect is negligible.

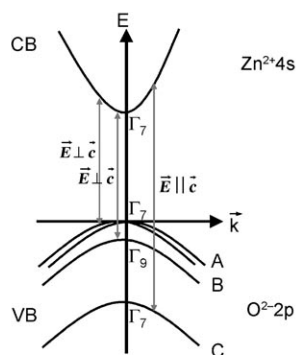

Figure 7. The valence band (VB) and conduction band (CB) of ZnO in the vicinity of the fundamental band gap.

6. Electrical Conductivity and Doping

The main problem for the application of ZnO as a material for electro-optic devices is ambipolar doping. This problem is frequently found for wide-band-gap materials and occurs when doping of one type (e.g. n-type conductivity due to electrons in the CB) is easily possible up to high densities, while the opposite type (in this case due to holes in the VB) is hardly achievable. The semiconductors ZnO, ZnSe, CdS or GaN are, for example, generally n-type while ZnTe is generally p-type. In this section, we first give information about the electron mobility in bulk samples, epilayers and quantum wells, and then we address the problem of n- and p-type doping.

6.1. Hall Mobility

In this subsection, we concentrate mainly on the Hall mobility, μ_H. Some data for the generally smaller drift mobility and the difference between the two quantities can be found in ref. [45]. In the past, the Hall mobility of electrons has been investigated many times for bulk samples.[45] In Figure 8, we show data from ref. [46], which have been confirmed recently,

 © 2007 Wiley-VCH Verlag GmbH & Co. KGaA, Weinheim

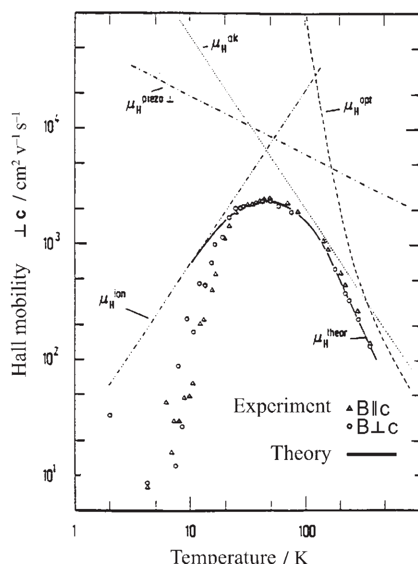

Figure 8. Temperature dependence of the Hall mobility of ZnO for $\boldsymbol{E}\perp\boldsymbol{c}$. From [46].

for example, in refs. [47–49]. As usual, the mobility at low temperatures is limited by scattering with ionised impurities, and, for $T \leq 10$ K, possibly even by hopping processes in an impurity band. With increasing temperature, the mobility goes through a maximum, with values around 2000 $cm^2V^{-1}s^{-1}$ and drops at higher temperatures to values between 200 and 400 $cm^2V^{-1}s^{-1}$ due to scattering with acoustic and optic phonons via deformation potential coupling, piezoelectric fields or Froehlich interaction (Figure 8).[48,49] Since these are intrinsic processes, one cannot expect a considerable increase of the room-temperature values by improved crystal growth. In thin films, epilayers and similar structures, one often finds lower values at room temperature, typically around or even clearly below 100 $cm^2V^{-1}s^{-1}$ because of scattering at grain boundaries or surface/interface roughness.[48,49]

Values up to 3100 $cm^2V^{-1}s^{-1}$ at room temperature reported for nanorods[50] may be either questionable or must involve the quenching of some of the intrinsic scattering processes due to the small lateral dimensions. Since the measurement of μ_H of a single nanorod is a nontrivial task, the author tends to the former explanation.

Data on the hole mobility in ZnO are still not very common. Values around 5–30 $cm^2V^{-1}s^{-1}$ have been reported, which are, as expected, lower than for electrons.[51]

With increasing strength of the field $\boldsymbol{E}$, the drift velocity starts to grow only sublinearly with $\boldsymbol{E}$ above a certain limit and possibly even goes through a maximum. Experimental and theoretical data of this high-field transport can be found in ref. [52].

In quantum wells, the concept of modulation doping can be realised. In this case, the donors are located in the $Zn_{1-y}Mg_yO$ barrier, and the electrons are captured in the ZnO quantum well (QW). In this way, the free carriers can be spatially separated from the ionised donors, thus reducing the scattering rate with these defects. As a result, low-temperature mobilities up to 2700 $cm^2V^{-1}s^{-1}$ have been reported in ZnO QWs.[53,54] Such values allow the obervation of the (integer) quantum Hall effect in ZnO. For first reports, see ref. [54].

6.2. n-Type Doping

For n-type doping, one would choose to substitute Zn or O with atoms which have one electron more in the outer shell than the atom which they replace. Consequently, the Group III elements Al, Ga, and In are shallow and efficient donors if they replace Zn according to Equation (2)

$$D^\circ \rightleftharpoons D^+ + e^- \tag{2}$$

where D° and D^+ are the neutral and ionised donors, respectively, and the equilibrium at room temperature is essentially on the right-hand side of Equation (2). Indeed, electron concentrations beyond 10^{20} cm^{-3} are obtained in ZnO:Al or ZnO:Ga, which even at room temperature result in a degenerate electron gas in the conduction band. For a few references including the UV and IR optical properties, see, for example, refs. [55,56]. A degenerate carrier gas is characterised by the fact that the Fermi energy (or chemical potential) is located in the band and no longer in the band gap and that consequently Fermi–Dirac statistics are mandatory for an adequate description. The limit between a description in terms of classical Boltzmann and degenerate Fermi–Dirac statistics is the so-called effective density of states, which for ZnO at room temperature is given by Equation (3):[10]

$$n_{\text{eff}} = 2\left(\frac{2\pi m_e k_B T}{h^2}\right)^{3/2} = 4 \cdot 10^{18} \text{cm}^{-3}. \tag{3}$$

At densities around 10^{20} cm^{-3}, the plasma frequency ω_{Pl}^0, given by Equation (4) for $\mathbf{k} = 0$:

$$\omega_{Pl}^0 = \left(\frac{ne^2}{\varepsilon_0 \varepsilon_b m_0}\right)^{1/2} \tag{4}$$

corresponds to photon energies $\hbar\omega_{Pl}^0$ of a few hundred millielectronvolts. Consequently, such highly doped samples show high reflectivity from $\omega = 0$ to the longitudinal energy $\hbar\omega_{Pl}^0$ situated in the near-IR with some peculiarities around optically active phonon modes (see above) due to the formation of plasmon–phonon mixed-state quanta.[56]

The other possibility for n-doping would be to use Group VII elements on the anion site. Though this combination is known to be very efficient, for example, for ZnSe:Cl,[57] it has been less thoroughly investigated for ZnO. Furthermore, it has been shown that hydrogen in ZnO is always a donor.[58] This might be, together with small deviations from stoichiometry, a reason that ZnO without intentional doping is always n-type.

6.3. p-Type Doping

According to the above rules, one would expect that the Group I elements Li, Na or K are good acceptors. Indeed Li, Na, K and also the Group I^b elements Cu and Ag are known to act

 © 2007 Wiley-VCH Verlag GmbH & Co. KGaA, Weinheim

as acceptors. However, they are usually deep acceptors with ionisation energies around a few hundred millielectronvolts,[59,60] that is, much larger than k_BT at room temperature. As a consequence, the equilibrium at room temperature is on the left-hand side of Equation (5).

$$A^{\circ} \rightleftharpoons A^{-} + \text{hole} \quad (5)$$

Therefore, ZnO:Li is a high-resistivity material but does not show p-type conductivity at room temperature. In addition, interstitial Li (or Ag) occurring at high doping levels may act as a donor, thus compensating part of the acceptors.[59] Samples grown by the hydrothermal technique from LiOH/KOH bases necessarily have a high incorporation of these cations. Consequently, they are high resistivity materials, and it is difficult to obtain good n-type doping for them. Recently, it has been claimed that Li or a complex involving Li may also form a shallow acceptor in ZnO.[61]

As a consequence of these problems, a lot of research presently concentrates on p-type doping with the Group V elements N, P or As on oxygen site. After a lot of poorly reproducible results and other problems, there were recently reliable reports on p-type doping in ZnO with N, As or P. Nitrogen is not incorporated in the ZnO lattice if it is offered as N_2 (e.g. during the growth in air). It is incorporated in the form of single atoms or ions, for example, from a nitrogen plasma source. The nitrogen acceptor has an even smaller ionisation energy (about 100 meV) than the standard acceptor Mg in GaN:Mg, with 160 meV. The doping level, generally below or around 10^{17} cm^{-3}, is still limited, as is partly the solubility of the Group V elements on O sites. Frequently, one finds orders of magnitude lower hole concentrations than the density of incorporated acceptor atoms. This means that only a small fraction of the incorporated atoms, such as N, forms the desired shallow acceptors, while the majority forms complexes or other defect states, which may partly even act as donors and compensate the acceptors, as mentioned above for ZnO:Li. This finding is supported by the fact that the p-type layers frequently show deep-centre luminescence, for example, in the orange or blue-green spectral ranges, as discussed below in conjunction with Figure 24.

It is hoped that some progress can be made by codoping, that is, by using either two different acceptors simultaneously (e.g. ZnO:N,As) or by combining a moderate concentration of donors with a higher concentration of acceptors (e.g. in ZnO:Ga,N). Furthermore, it has been found that Li may form a complex in ZnO with a relatively low ionisation energy of 130 meV.[61]

7. Deep Centres

While efficient donors or acceptors have energy levels close to the conduction or valence band, respectively, there are also deep centres with levels energetically deep in the forbidding gap. We have already mentioned deep acceptor levels situated energetically a few hundred millielectronvolts above the valence band. The light emission resulting from the recombination of a free electron in the conduction band with a hole bound, for example, to a Li acceptor is therefore situated in the yellow spectral range, while the intrinsic luminescence processes result in blue or near-UV emission, as we shall see in Section 9. There are many other deep extrinsic centres known in ZnO, such as Cu, Fe, Co, Mn or OH, to name a few, and intrinsic ones such as oxygen vacancies or zinc intertitials. Concerning the optical properties, deep centres may lead to additional absorption bands. ZnO:Cu or ZnO:Co show, for example, different green colours. Concerning the light emission, deep centres may lead to emission bands at photon energies significantly below the gap, either because of free-to-bound transitions, such as the yellow emission of ZnO:Li mentioned above, or owing to internal transition within the centre, such as the green emission in ZnO:Cu. In Figure 9, we show an overview of various emission bands. Red emission results from ZnO:Fe; green emission can come from Cu centres or from oxygen vacancies. Such deep-centre luminescence makes it possible to obtain light emission from ZnO that is not only close to the intrinsic absorption edge, which is in the near-UV, but also over the whole visible spectrum. For a few of the many papers on deep centres in ZnO, see refs. [9, 59, 62–64].

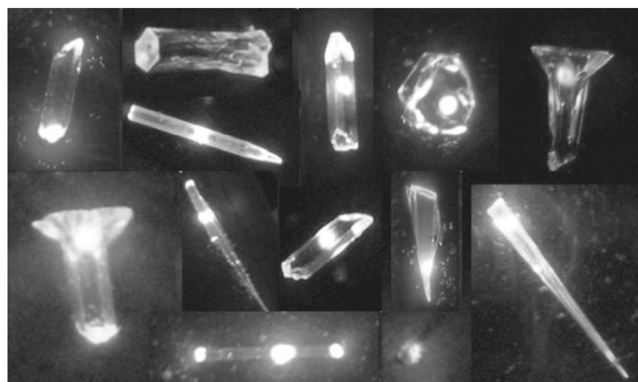

Figure 9. Deep-centre luminescence of various ZnO samples. The colour version on the front page of this review shows emission in various regions of the visible spectrum.[14]

In ZnO powders, an external luminescence yield at low temperatures up to several tens of percents has been determined for a green luminescence band.[65]

However, it should be mentioned that some deep centres, such as Cu or Fe, may also act as luminescence killers at higher concentrations.

8. Magnetic Properties

A topic that results in a wealth of beautiful physical phenomena are so-called diluted-magnetic or semimagnetic semiconductors (DMSs). These are, for example, semiconductors that are doped or alloyed with a substantial fraction (from 1% to around 10%) of magnetic ions such as Mn, Fe, Co, V and so on. Due to the coupling of the spins of free carriers with the spins of the magnetic ions, surprising effects can be observed,

 © 2007 Wiley-VCH Verlag GmbH & Co. KGaA, Weinheim

such as a giant Zeeman splitting with g-values around 100 in $Zn_{1-x}Mn_xSe$ or the formation of magnetic polarons. These polarons are free electrons, which carry with them a cloud of aligned spins of the surrounding magnetic ions. Some of the DMSs, such as ZnO:Co and ZnO:Mn, exhibit ferromagnetism up to room temperature. In Figure 10, we show as an example

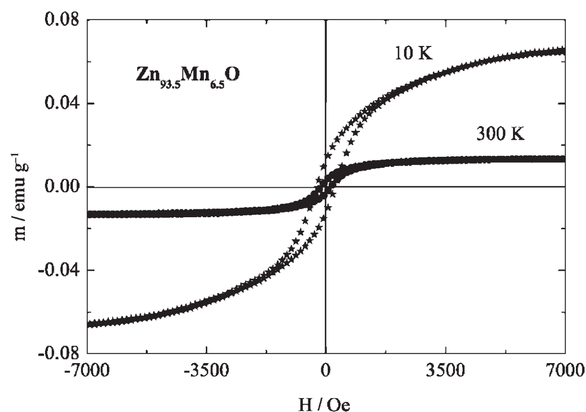

Figure 10. Ferromagnetic hysteresis loops of Mn containing ZnO for two different temperatures. From [66].

the hysteresis loop of a $Zn_{1-x}Mn_xO$ film at low temperature and at room temperature. Currently there is a vivid and controversial discussion concerning to what extent this ferromagnetism is due to the doped ZnO:X (X = Mn, Co, V,...) matrix itself or to clusters or precipitates of other phases.[66,67] The absence of additional peaks in X-ray diffraction (XRD) experiments turned out not to be sufficient to rule out secondary phases. See the work by H.-J. Lee and by H. Zhou in ref. [67]. Some theoretical models predict room-temperature ferromagnetism in DMS ZnO only for unrealistically high p-doping levels.[66,67]

The magnetisation is frequently given in the rather strange "electromagnetic units" (emu) or in emu g.$^{-1}$ Typical values are in the range of 10^{-2} to 10^{-5} emu. The following relation holds between the various units of the magnetic field [Eq. (6)].

$$1\ \mathrm{emu} = 10^{-3}\ \mathrm{A\,m^{-1}};\ 1\ \mathrm{A\,m^{-1}} = 4\pi 10^{-7}\ \mathrm{V\,s\,A^{-1}m^{-1}} = 4\pi 10^{-7}\ \mathrm{T} \quad (6)$$

Consequently, the magnetic field connected with a ferromagnetic DMS is orders of magnitude below the magnetic field of the earth, which is a few tens of microtesla. Though DMSs allow performing beautiful physics in experiment and theory, these numbers (and not only these) cast some serious doubts on the highly speculative concept of semiconductor spintronics and even more on the field of quantum computing. The author feels that this aspect is not only relevant for the II–VI DMSs.[10]

9. Linear Optical Properties

We have mentioned the optical properties connected with optical phonons and with plasmons in highly doped samples and the resulting plasmon–phonon mixed states in Sections 3 and 6 and the properties of deep centres in Section 7. In this section and in the following sections, we concentrate on the electronic optical properties close to the fundamental absorption edge, which in ZnO, as already mentioned in the introduction, is in the blue/near-UV range.

9.1. Free Excitons and Exciton Ppolaritons

The simplest way to describe the expected absorption spectrum in a direct-gap semiconductor with a dipole-allowed band-to-band transition like ZnO is in terms of these band-to-band tranitions as shown in Figures 7 and 11 a. A photon with an energy larger than the band gap excites an electron from the VB to the CB. Since the density of states varies in three dimensions for a parabolic $E(\mathbf{k})$ relation as the square-root with the energy, one would expect, on this level, the onset of the absorption spectrum $\alpha(\hbar\omega)$ according to Equation (7):

$$\alpha(\hbar\omega) \propto \begin{cases} \sqrt{\hbar\omega - E_g} & \text{for } \hbar\omega \geq E_g \\ 0 & \text{otherwise} \end{cases} \quad (7)$$

Indeed, this picture is too simple to be compatible with reality. We see from Figures 7 and 11 a that an absorption process is a two-particle transition, that is, by the absorption of a photon, an electron in the CB and a hole in the VB are created

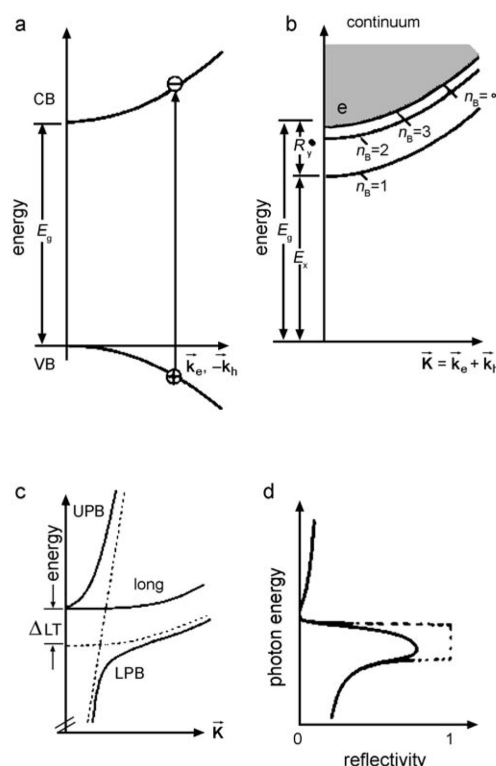

Figure 11. Schematic drawing of a) the band-to-band transition and b) the resulting exciton states. c) The exciton polariton resulting from the coupling of the exciton with light, and d) the reflection spectrum of such a resonance.[10]

 © 2007 Wiley-VCH Verlag GmbH & Co. KGaA, Weinheim

simultaneously. Similarily, two particles are annihilated in a radiative or nonradiative recombination process.

The point is now that electron and hole interact via their attractive Coulomb potential, forming a series of hydrogen- or positronium-like states below the gap (Figure 11 b). These states are called excitons or more precisely Wannier excitons, which are characterised by the fact that the average distance between electron and hole, that is, the excitonic Bohr radius a_B, is larger than the lattice constant, in contrast to so-called Frenckel excitons, which occur in insulators or organic crystals and in which electron and hole reside in the same unit cell.

The excitons are, generally speaking, the quanta of the excitation in the electronic system of semiconductors or insulators. The ground state for the first case is a semiconductor with completely filled VB and empty CB. It has energy $E=0$ and total momentum $\hbar\boldsymbol{k}=0$. The series of hydrogen-like exciton states with main quantum number $n_B=1, 2, 3,\ldots$ is followed by the ionisation continuum, starting at E_g. For all the exciton series resulting from the transitions from the A, B, and C VB (Figure 7) into the CB, the excitonic binding or Rydberg energy (E_x^b or R_y*) in ZnO is $E_x^b \approx 60$ meV. The excitonic Bohr radius of ZnO is $a_B=1.8$ nm. The translational mass is given by the sum of effective electron–electron and electron–hole masses. The deviations from the data of hydrogen are caused by the effective and reduced electron and hole masses and the dielectric constant. The band structure (Figure 11 a) and the exciton states (Figure 11 b) must not be drawn in the same diagram, because the former are one-particle states and the later two-particle states.

If we go one step further in the discussion of the optical properties, we come to the polariton concept. The dashed lines in Figure 11 c give the dispersion of the $n_B=1$ exciton and of the photon. If there is a coupling between the two, that is, if the transition from the crystal ground state to the exciton is optically (dipole-) allowed, there is an avoided crossing, resulting in the dispersion curve given by the solid line. This solid line is the dispersion curve $E(\mathbf{k})$ of the mixed or coupled state of exciton and photon and is known as the exciton polariton. The dispersion of the lower polariton branch (LPB) starts photon-like, then bends over to an exciton-like behaviour. There is a finite transverse-longitudinal splitting Δ_{LT}; there may be a longitudinal eigenmode, and above the dispersion, the upper polariton branch (UPB) bends over again to photon-like behaviour. The dashed lines in Figure 11 c serve only for the construction of the polariton dispersion. They do not correspond to any real states in the crystal.

In Figure 11 d, we show the reflection spectrum of an exciton polariton resonance (solid line). Due to the curvature of the LPB, for every energy there is at least one propagating polariton mode in the sample. Consequently, the reflectivity does not reach unity as expected for a stop band without damping (dashed line). Exciton states, which do not couple to the light field because of the selection rules, remain pure excitons.

The exciton or exciton-polariton states can be excited directly by photons according to the selection rules. The absorption spectrum at low temperature resulting from the exciton series and the ionisation continuum consists of a series of relatively sharp absorption bands for the exciton or excitong-polariton states with $n_B=1, 2, 3,\ldots$ with a width given either by Δ_{LT} or by the homogeneous width, whatever is larger. At higher energies comes absorption into the ionisation continuum, starting at E_g. At higher temperatures, there is scattering with phonons and a resulting stronger homogeneous broadening. This broadening results in an exponential tail of the absorption, which, with increasing temperature, extends more and more to lower energies, according to the Urbach–Martienssen rule.[10] In Figure 12, we show various optical spectra of excitons in ZnO. Figures 12 a and b show the A, B, and C $n_B=1$ exciton resonances in reflection in their respective polarisation (Figures 7 and 11 d). Figure 12 c shows an early room-temperature absorption spectrum of a thin ZnO film. The A and B exciton resonances merge to the peak around 3.3 eV. It should be noted that in the excitonic ionisation continuum of ZnO, the absorption coefficient reaches values beyond 10^5 cm^{-1}. In the exciton resonances, it is higher still and correspondingly difficult to measure, especially at low temperatures, where the broadening is smaller.

Finally, in Figures 13 a–c, we show the excitonic luminescence spectra of ZnO for various temperatures. One sees the (broadened) peak of the A and B exciton polaritons at 110 K around 3.37 eV and their longitudinal-optical (LO) phonon replica around 3.30 eV and 3.225 eV. With increasing temperature, the homogeneous broadening increases, as mentioned above, resulting at room temperature (and above) in a broad, unstructured emission band. This band is seen in bulk samples, epitaxial layers, and nanorods. It should be noted that its peak is not identical with the exciton energy. The discrepancy between measured spectra and models at higher temperatures results from reabsorption. Investigation of absorption and luminescence allow the determination of the temperature dependence of the free exciton resonances (and also of the band gap). In Figure 13 d, we show this dependence up to 800 K. The damping deduced from the line-shape fit shows that the homogeneous broadening of the exciton resonance increases from values below 1 meV at 5 K to 20 meV (half-width-at-half-maximum) at room temperature.

In Figure 13 a, one observes sharp emission peaks around 3.35 eV. This is the reminder of bound exciton complexes described in the following section.

9.2. Bound Exciton Complexes

In the preceding section, we treated the optical properties of free, intrinsic excitons and excition polaritons, which are characterised by a $\boldsymbol{k}$ vector and a dispersion relation $E(\mathbf{k})$, and which can move freely through the crystal and are subject to scattering processes, for example, with phonons or structural defects. Furthermore, excitons can be bound to some centre or defect, like ionised or neutral donors (D^+, D^0) or neutral acceptors (A^0), thus forming D^+X, D^0X or A^0X bound-exciton complexes (BEC).[69] These BEC have no translational degrees of freedom. Therefore, at low temperatures they form very narrow luminescence and absorption bands. In good samples, they have a width below 1 meV. In Figure 14, we show a low-

 © 2007 Wiley-VCH Verlag GmbH & Co. KGaA, Weinheim

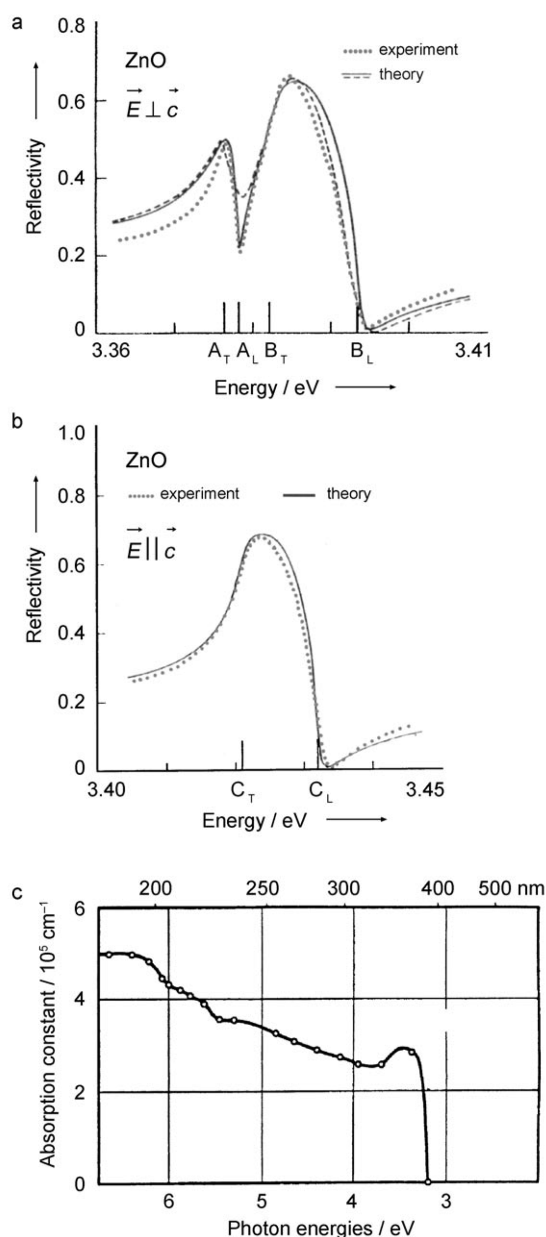

Figure 12. a) Reflection spectra of the $n_B=1$ A, and B exciton-polariton resonances at 1.8 K (••••• experiment; —— and – – – theoretical modelling using two different appoaches). b) Reflection spectra of the $n_B=1$ C exciton-polariton resonances at 1.8 K (••••• experiment; —— theoretical modelling).[6] c) A room-temperature absorption spectrum.[3,28]

temperature luminescence spectrum of a high-quality ZnO bulk sample. One observes the free-exciton emission (FE) as a rather weak line at 3.375 eV together with its first LO-phonon replica at 3.303 eV. The BEC are situated in the interval from 3.35 to 3.37 eV. D^+X have the smallest binding energy to the complex (about 5 meV), which for D^0X ranges from 10 to 20 meV; the deepest line at 3.354 eV might be due to an A^0X complex. The BEC, together with their LO-phonon replica (here at 3.29 eV) and the so-called two-electron transitions (at 3.32 eV), generally dominate the luminescence spectra of semiconductors at low temperature close to the intrinsic absorption edge. With increasing temperature, the excitons are more and more thermally released from their centres and tend to disappear around 80 K in ZnO (see Figure 13).

The lifetimes of free and bound excitons in ZnO, as in other direct wide-gap semiconductors, are typically in the range of 0.3–1 ns and, especially for the free excitons, are generally determined by nonradiative recombination processes. This statement can be deduced from the fact that the absolute external luminescence yield of the free and bound excitons, including their LO-phonon replica, is considerably below unity, with values around or below 10% in high-quality samples.[65]

10. High Excitation Effects

When one increases the densities of excitons and/or free carriers in an semiconductor, for example, by excitation with short and intense laser pulses or by carrier injection in a forward-biased p(i)n-junction, new phenomena appear in the optical spectra.

The scenario was developed in the 1980s. It is didactically very valuable, and we first outline it here shortly and, in Section 11, then add the modifications necessary from the current viewpoint. As we shall also see in Section 11, many of the effects introduced here are capable of showing stimulated emission. In Figure 15, we show a schematic depiction of a sample and the processes which occur with increasing generation rate or excitation intensity. In the low-density limit (e.g. under quasistationary excitation conditions), there are free excitons; at low temperature there are also bound exciton complexes, and at higher temperatures there are also some free carriers resulting from either the thermal ionisation of excitons or of donors, since undoped ZnO is usually an n-type semiconductor.

At intermediate densities, we enter into the regime of nonlinear optics with new emission processes. The intermediate-density regime is ideally characterised by the fact that excitons are still good quasiparticles. If two excitons meet during their lifetime on their diffusive path through the sample, various things can happen. They can scatter elastically under energy and momentum conservation, resulting in a density-dependent increase of their damping or homogeneous line width. Or they can scatter inelastically; in this process, one exciton or exciton polariton is scattered into a higher state with $n_B=2, 3,\dots$ or into the continuum, while the other is scattered down onto the photon-like part of the dispersion relation and leaves the sample as a luminescence photon. The corresponding emission bands (known as P_2 or P_∞ bands) are broadened due to the thermal distribution of excitons in their bands in addition to homogeneous broadening. See Figure 16 for a schematic drawing of the inelastic exciton–exciton scattering (X–X) process and its observation in the luminescence spectrum.

The X–X process has been observed in many semiconductors;[10] for ZnO, see, for example, refs. [70–72,77].

Energy and momentum conservation lead to Equation (8):

$$\hbar\omega_{P_n} = E_x(n_B = 1, \vec{\mathbf{k}} = 0) - E_x^b(1 - \frac{1}{n_{B_f}^2}) - \frac{\hbar^2}{M}\vec{\mathbf{k}}_{i_1}\vec{\mathbf{k}}_{i_2} \quad (8)$$

where E_x on the right hand side gives the exciton ground

 © 2007 Wiley-VCH Verlag GmbH & Co. KGaA, Weinheim

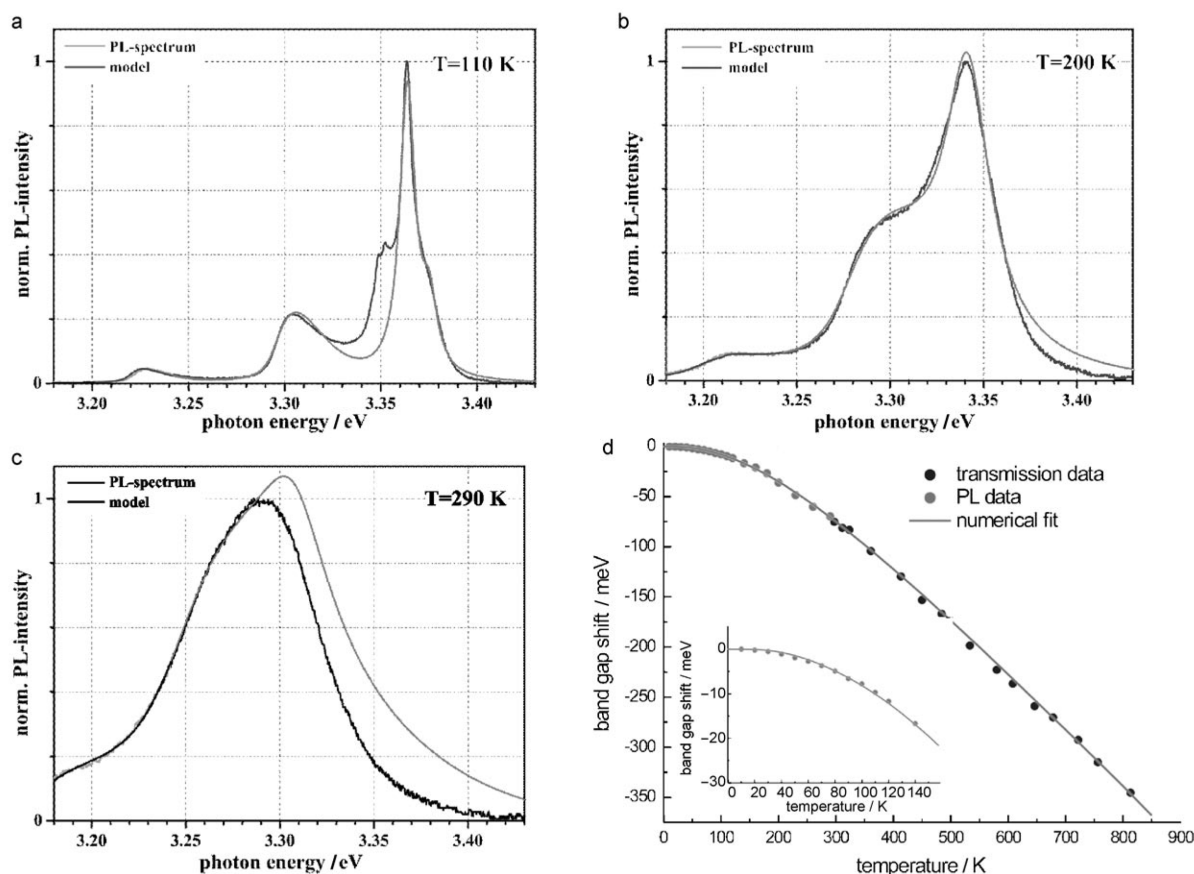

Figure 13. a)–c) Luminescence spectra of ZnO for various temperatures. —— measured spectra; —— model. d) Temperature dependence of the band gap; the inset shows an expansion of the temperature range 0–150 K. PL = photoluminescence.[68]

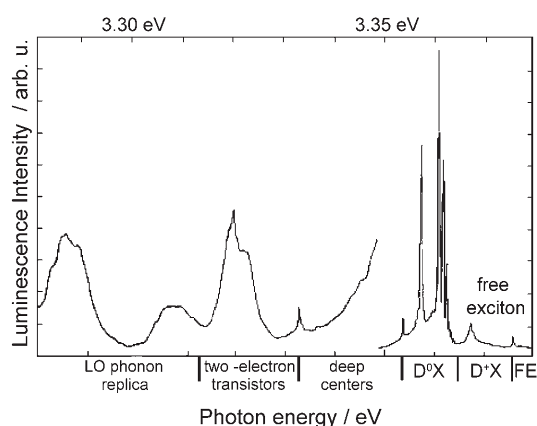

Figure 14. Low-temperature (1.8 K) luminescence of a ZnO bulk sample in the range of free and bound excitons and their LO-phonon replica. From Tomzig and Helbig in ref. [69].

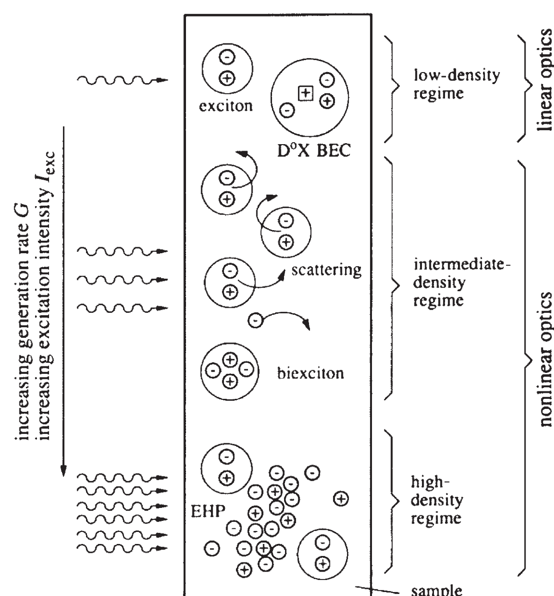

Figure 15. Schematic drawing of the scenario in a semiconductor with increasing excitation.[10] EHP = electron-hole plasma.

state, $M = m_e + m_h$ is the translational exciton mass and $\vec{\mathbf{k}}_{i_1}$ and $\vec{\mathbf{k}}_{i_2}$ give the wavevectors of the two excitons in the initial state. The thermal average over the last term on the right-hand side of Equation (8) can be approximated by $3\delta k_B T$ with $0 < \delta < 1$. At low temperatures, Equation (8) results in values around 3.32 eV for P_∞. In Figure 17, we show normalised emission spectra for low temperature and increasing excitation density of a 0.4-μm thick epitaxial ZnO layer grown by MOVPE on $Al_2O_3(111)$ with a GaN buffer layer. The lowest trace has been

 © 2007 Wiley-VCH Verlag GmbH & Co. KGaA, Weinheim

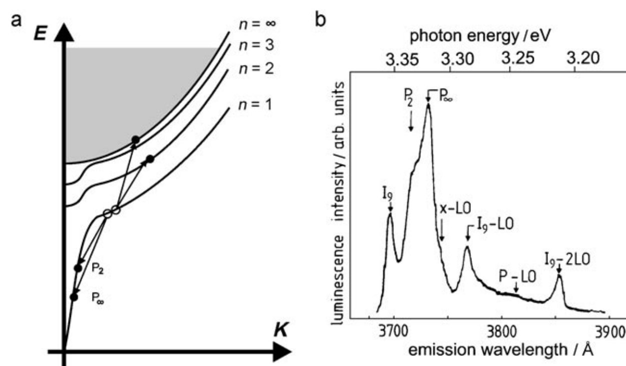

Figure 16. a) Schematic drawing of the inelastic exciton–exciton scattering process. (a) and its b) Observation of the scattering process shown in (a) as P_2 and P_∞ bands in the luminescence spectrum of ZnO at 10 K.[10,70]

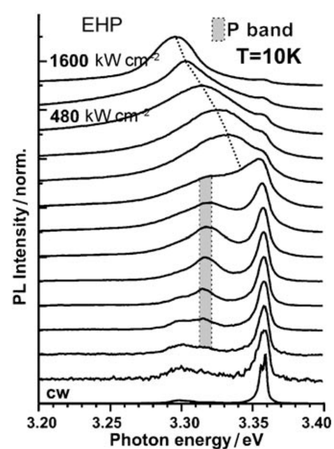

Figure 17. Normalised luminescence spectra of a ZnO epitaxial layer at low temperature and for increasing excitation.[72]

taken under continuous wave (cw) excitation with a HeCd laser ($\hbar\omega_{exc}=3.81$ eV) and shows essentially the dominant BEC luminescence (see Section 9.2). At intermediate pump powers, the P band appears around 3.32 eV.

Another process which can occur at low temperatures during the collision of two excitons is the formation of an excitonic molecule or biexciton, in analogy to the formation of an H_2 or a positronium molecule. The binding energy E^b_{xx} of the biexciton relative to two free excitons is in ZnO around 15 meV.[73] This binding energy must be dissipated in the biexcitonic formation process from two free excitons in the form of phonon (or photon) emission. Since E^b_{xx} is larger than the splitting of the A and B VBs, in ZnO, the biexciton states which contain one hole from the A and one from the B VB or even two B holes are also observed. The binding energies of these states are similar, relative to the two involved excitons.[12,73] Biexcitons have also been observed in ZnO QWs, see, for example, ref. [12]. The binding energies of both excitons and biexcitons are enhanced in QWs due to the spatial confinement in one direction.

Apart from the formation in an collision between two free excitons, biexcitons can be created directly by two-photon absorption starting from the crystal ground state or by the conversion of an exciton into a biexciton by absorption of one photon.[7,8,10] This latter process is called induced absorption. It occurs at a photon energy given by Equation (9)

$$\hbar\omega_{ia} = E_x - E^b_{xx} - \frac{\hbar^2 \vec{\mathbf{k}}_i^2}{4M} \tag{9}$$

where $\hbar\mathbf{k}_i$ is the momentum of the initial exciton and it has been assumed that the effective mass of the biexciton is twice the exciton mass M. In luminescence, one generally observes the inverse process, that is, the decay of a biexciton into an exciton and photon or photon-like polariton appearing in luminescence (Figure 17). This emission band is usually called the M band. It occurs spectrally in the range of the A^0X or D^0X BEC, since all three complexes consist of two heavy positive and two light negative charges. As a consequence, other explanations of the M band have been developed, such as the radiative recombination of a BEC under emission of an acoustic phonon or under scattering with a free carrier.[7] In Figure 17, we see the M band at higher excitation (around 3.36 eV). The M band dissappears from the luminescence spectra, as does the BEC, at higher temperatures, because the biexciton is thermally dissociated.

At even higher temperatures ($T \geq 100$ K), when excitons themselves are partly thermally ionised, another inelastic scattering process sets in between excitons and free carriers (X–el), in ZnO generally electrons. This process is shown schematically in Figure 18. A thermal distribution results, as indicated in a

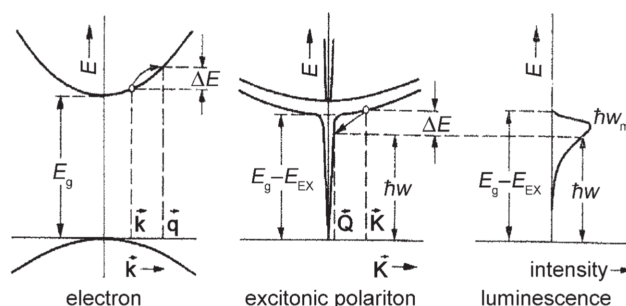

Figure 18. Schematic drawing of the inelastic exciton-electron scattering. The wave vectors $\vec{K}$ and $\vec{k}$ refer to exciton polariton and electron in the inital, $\vec{Q}$ and $\vec{q}$ in the final states, respectively.[7,10,71]

rather broad emission band with the characteristic property that, with increasing temperature, its maximum shifts considerably faster to lower energies than the band gap does. Again, this fact results essentially from energy and momentum conservation.[7,8,10,71]

In Figure 19, we show the temperature dependences of the emission maxima of various recombination processes. The experimental data for the X–X and X–el processes are indicated by dashed lines.

At the highest densities, the excitons cease to exist as individual quasi-particles, and a new collective phase of Coulomb-

 © 2007 Wiley-VCH Verlag GmbH & Co. KGaA, Weinheim

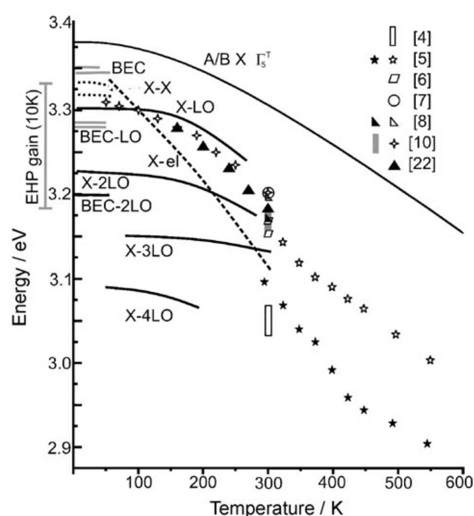

Figure 19. Temperature dependence of the energy of the transverse $n_B=1$ Γ_5 A and B excitons and of various emission maxima.[71,74] The references [4–8, 10, 22] in the figure correspond to refs. [79–85] of this paper. The open symbols stand for X–X scattering , the closed ones for EHP recombination (see text for details).

correlated electrons and holes is formed, the so-called electron-hole plasma (EHP; see bottom of Figure 15). The transition from an insulating gas of neutral excitons to the metallic state of an EHP is also known as the Mott transition occuring at the Mott density n_M. In direct-gap materials, the transition is generally smooth and not abrupt.[10,78] The calculation in Figure 20a gives the energies in units of the excitonic Rydberg or binding energy $R_y{}^*=E_x^b$. The calculation is for CdS. The results are similar for ZnO, but n_M is at $n_p=5\times10^{17}\,cm^{-3}$ instead of $8\times10^{16}\,cm^{-3}$.[78] This Mott transition is caused by the following many-particle effects. The width of the forbidden gap is a monotonously decreasing function with increasing electron-hole pair density n_P, due to exchange and correlation effects. The binding energy of the exciton $E_x^b(n_P)$ also decreases with increasing n_P, because the Coulomb attraction of electron and hole is increasingly screened by the additional electron–hole pairs and vanishes at n_M. As a consequence, the absolute energy of the exciton $E_x=E_g(n_P)-E_x^b(n_P)$ is almost constant, but its damping increases with n_P. In ZnO, n_M is around $5\times10^{17}\,cm^{-3}$ and only weakly dependent on temperature. In Figure 20, we show this behaviour schematically. In the upper spectra of Figure 17, emission from an EHP is seen. The increasing redshift of the emission with increasing excitation reflects the decrease of $E_g{}'$ with increasing n_P, and the narrowing of the emission band indicates the onset of stimulated emission. This aspect brings us to the topic of the next section.

11. Stimulated Emission

In this section, we treat first the basic concepts of stimulated emission in ZnO, and then we refine the picture as announced in Section 10.

11.1. Basic Concepts

All of the excitonic interaction processes introduced above, as well as some others, are capable of showing stimulated emission.[7,8,10] For early reports on stimulated emission in ZnO, see, for example, refs. [70,71,76,77]. Generally, excitonic interaction processes can be mapped on a four-level laser system. Since the lower level of the laser transition is not populated or only weakly populated (in contrast to a three-level laser system, where the ground state is identical with the lower level of the laser transition), population inversion is easily reached. We illustrate this statement with two examples. In the X–nLO process, an exciton recombines radiatively under emission of a photon and one (or more) LO phonons (Figures 13 and 19). This process can be stimulated. It is inverted in principle if there is one exciton in the sample and no LO phonon (situated around 72 meV, see Section 3) that is, at low temperatures. To overcome finite losses, one needs, of course a finite density of excitons for laser emission. Since LO phonons tend to decay rapidly into lower-energy phonons, the lower laser level, (the

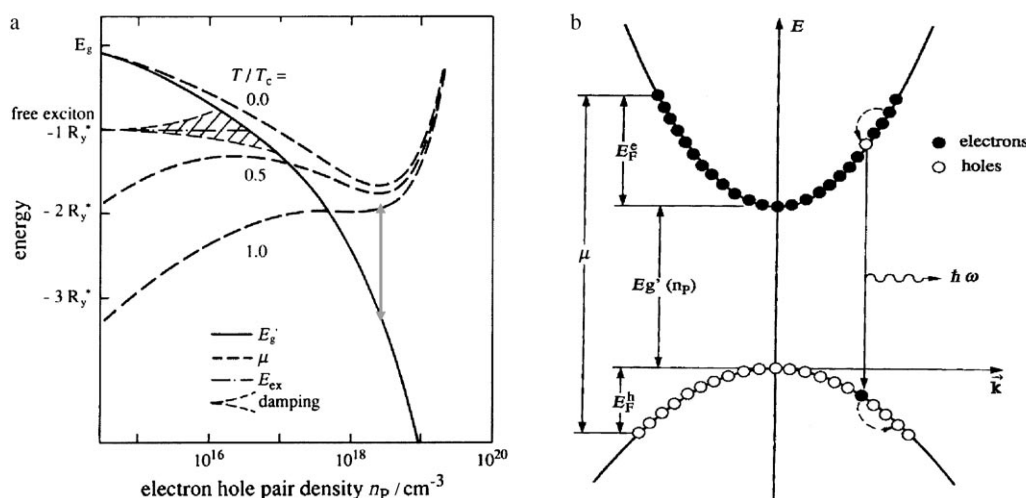

Figure 20. The band-gap renormalisation, the energy of the free exciton and its damping and the chemical potential μ of the electron-hole pair system as a function of the electron-hole pair density (a) and the recombination in a degenerate, inverted electron-hole plasma (b). From [75] and [10], respectively.

 © 2007 Wiley-VCH Verlag GmbH & Co. KGaA, Weinheim

LO phonon state) remains weakly populated at low temperatures. At higher temperatures, the LO-phonon state becomes thermally populated and reabsorption occurs both by the reverse process and by the temperature-dependent absorption tail of the exciton (Figure 13 c). Eventually, the stimulated emission goes over from the first LO-phonon replica to the second one at temperatures around 100 K.[76] In Figure 21, we show the luminescence intensities of the first three LO-phonon replica of the A and B excitons as a function of the generation rate in this transition region. The threshold behaviour of the first two is obvious.

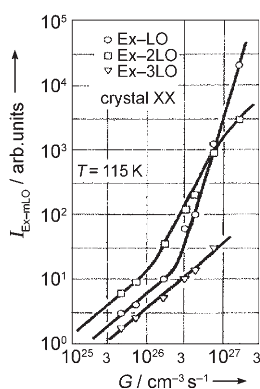

Figure 21. The dependence of the luminescence intensity on excitation, that is, on the generation rate G for the first three LO-phonon replica under two-photon excitation in ZnO at 115 K.[71, 76]

sities. The creation of an EHP is connected with the disappearance of the excitonic features in the reflection spectra as reported, for example, in ref. [78]. It must be noted that the density to reach population inversion n_{pi} is given by the above-mentioned intersection of $\mu(n_P,T)$ with $E_g'(n_P)$ and, especially at higher temperatures, is considerably higher than the Mott density n_M introduced in Section 10. In Figure 20 a, the double arrow indicates the spectral interval in which optical amplification occurs. In Figure 22 spectra of the optical gain are shown, which have been deduced from a variation of the excitation stripe length at various excitation intensities.

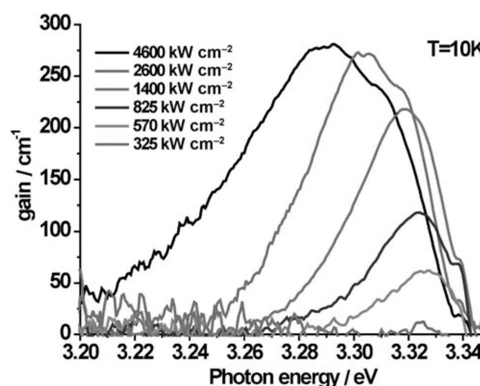

Figure 22. Spectra of the optical amplification (gain) in an EHP in an epitaxial ZnO layer.[72] Compare to the vertical solid line on the left-hand side of Figure 19, which gives the maximal spectral width of the gain in an EHP.

Similarily, the X–X emission bands are inverted if there are two excitons in the sample and none of them are in a state $n_B = 2, 3, \dots$ or in the continuum. The spectral positions of the P_2 and P_∞ bands are also given in Figures 17 and 19. With increasing temperature, higher exciton states also become populated and reabsorption sets in. Furthermore, the increasing ionisation of excitons favours the monopole-dipole interaction of the X–el process over the dipole–dipole interaction of X–X scattering, which is usually not observed in stimulated emission in bulk samples above 100 K. Around 100 K the X–X, X–LO and X–el processes are spectrally almost degenerate (Figure 19). As a rule of thumb, one finds that the stimulated emission frequently occurs not at the maximum of spontaneous emission but at lower photon energies, where reabsorption is less pronounced. This is especially true for broad emission bands like the one due to X–el scattering.

At the highest densities, the stimulated emission converts to recombination in an inverted EHP. In this case, inversion means that the energetic distance of the quasi-Fermi levels E_F^e and E_F^h, which describe the population of electrons and holes in their respective bands away from thermal equilibrium, must be larger than the reduced gap $E_g'(n_p)$. This distance is identical with the chemical potential of the electron–hole pair system $\mu(n_p,T)$ as shown in Figures 20 a, and b. This chemical potential μ is shown in Figure 20 a by the dashed lines. The lowest curve corresponds to $T \approx 65$ K . With further increasing temperature, the intersection of $\mu(n_P,T)$ with $E_g'(n_P)$ shifts to even higher densities.

Which of the above laser processes reaches the laser threshold first with increasing pump power depends on various parameters, such as the sample temperature, the loss rate that has to be overcome, the doping level and others. Most of the presently available commercial laser diodes work on the stimulated emission from an inverted EHP.

11.2. Refined Modelling

The processes introduced in Section 10 and above "for didactical purposes" have their right. The excitonic processes are realised for densities n_p considerably below n_M and for temperatures where the homogeneous broadening is small compared to E_x^b, that is, typically below room temperature. For possible future application of ZnO as a material for laser diodes (LDs), the processes at or even above room temperature are most relevant. Consequently, many research groups concentrate on this temperature range and preferentially investigate epitaxial ZnO layers. Surprisingly, the observed stimulated emission is attributed either to the X–X process, even partly specifying P_2 or P_∞, or to recombination in an inverted EHP. For some examples of these statements, see Figure 19 and references therein, where the open symbols stand for the claim of X–X scattering, the closed ones for EHP recombination. Experimentally, all room-temperature data for stimulated emission in ZnO are concentrated in the spectral range (3.15 $\pm$ 0.01) eV, irrespective of the claimed recombination process. The author feels that

 © 2007 Wiley-VCH Verlag GmbH & Co. KGaA, Weinheim

these statements for the origin of stimulated emission are, in many cases, not well-justified:

The nanosecond or picosecond pump or excitation intensities (for nanosecond pulses typically in the range from below 100 kWcm^{-2} up to 1 MWcm^{-2}) result in electron–hole pair densities between 10^{17} and 10^{18} cm^{-3} using realistic values of lifetime, penetration depth of the exciting light and diffusion length of the excited carriers.[74]

These values are close to or even above n_M, so that excitons are no longer good quasiparticles, because their binding energy tends towards or is already zero (Figure 20a). This makes the X–X process, that is, the P_2 or P_∞ bands, unlikely to explain room temperature lasing. Indeed, the P bands have been observed in bulk samples only for temperatures below about 100 K. On the other hand, these values of n_p, though partly above n_M, are too low for an inverted EHP at room temperature or above. Population inversion in an EHP occurs only around $n_{pi} \approx 10^{19}$ cm^{-3} at room temperature and at even higher densities above [Eq. (3)].

The large shift of the emission band denoted by the solid stars in Figure 19 relative to the band gap at 550 K would require values of $n_{pi}(550\,K) > 10^{20}$ cm^{-3}, which are above the damage threshold of the sample under nanosecond-pulse excitation and are incompatible with the excitation conditions.

Consequently, we have to look for alternative processes to explain the stimulated emission in ZnO at and above room temperature. The processes which we suggest[74] are in some sense modifications of the ones introduced above. One is an inelastic scattering of an essentially unbound electron–hole pair in an EHP and a free carrier, resulting in a photon and the free carrier scattered to higher kinetic energy. This process allows us to explain optical gain in an EHP for densities below n_{pi}. Energy and momentum conservation for this process also result in an enhanced redshift with increasing temperature, and the experimental data given by the solid stars in Figure 19 indeed extrapolate those for X–el scattering from lower temperatures. This is also true for the data for ZnO QWs.[85] Furthermore, it should be noted that the densities reached or claimed in older work at lower temperatures might have, in some cases, also been close to n_M, favouring the (electron–hole)–el process over the X–el process.[70,71,76,77]

For the next process, it should be noted that in the carrier gas of electrons and holes of an EHP, a new quasiparticle exists, the plasmon at energy $\hbar\omega_{Pl}$. This plasmon is a longitudinal eigenmode (the transverse frequency is zero), which interacts strongly with the optical phonons, resulting in still another quasiparticle, the plasmon–phonon mixed-state quantum.[10] This coupling effect is especially pronounced if $\hbar\omega_P$ is approximately equal to or even larger than $\hbar\omega_{LO}$. In ZnO, this is the case for $n_p \approx 3 \times 10^{18}$ cm^{-3}. Therefore, we introduce, as another process to explain lasing at room temperature and above, the recombination of an electron–hole pair in an EHP under emission of one or two plasmon–phonon mixed-state quanta. Since around n_M the reduced gap coincides with the energy of the exciton at low densities, at room temperature, this process also leads to emission in the above-mentioned interval but will shift less to lower energies with increasing temperature. We think that these processes are indeed good candidates to explain stimulated emission at room temperature and above (see the open stars in Figure 19), and partly also below. It is now a challenge to theory to model these processes quantitatively and by doing so to verify or falsify the above models.

11.3. Lasing in ZnO Nanorods and Powders

To conclude this section on stimulated emission and lasing, we mention that these phenomena have not only been observed in bulk samples, epitaxial layer or quantum wells as discussed avove, but also in ZnO nanorods and powders. For stimulated emission in nanorods, see, for example, refs. [86,88]. The discussion concerning the laser processes from Section 11.2 also applies here. In addition, the emission is strongly influenced by the cavity modes. Whispering gallery modes in nanorods have been investigated without laser emission in the broad green band,[87] mentioned in Section 7. The transverse and longitudinal mode pattern of nanorods has been calculated in ref. [88], and it has been found that the mode pattern has strong influence on the photon energy at which stimulated emission occurs.

Usually, one does not expect lasing in disordered media, but one expects the combination of a resonator and an active medium. Recently, however, it has been shown that so-called random lasing can occur in powders, for example, of ZnO.[89] The multiple scattering from the grains of the powder keeps the light in the pumped volume longer. This effect may even be enhanced by weak localisation of light in the random medium (i.e. the powder) by enhanced backscattering.

12. Applications of ZnO

ZnO is produced at levels of 10^5 tons per year. Zn is evidently much more available (and less poisonous!) than, for example, Ga. In the following, we give first a list of a variety of existing applications and then an outlook or vision for future applications, especially in the field of optoelectronics, including junctions.

12.1. Existing Applications

A large fraction of the ZnO currently produced is used in the rubber and concrete industries.[2] ZnO is an important additive to the rubber of car tyres. It has a positive influence on the vulcanisation process, and it considerably improves the heat conductivity, which is crucial to dissipate the heat produced by the deformation when the tyre rolls along the street. In concrete, an admixture of ZnO allows an increase in the processing time and improves the resistance of concrete against water. Other applications concern medicine or cosmetics. ZnO is used as an UV-blocker in suntan lotions or as an additive to human and animal food. Furthermore, it is used as one component of mixed-oxide varistors, devices which allow voltage limiting.

Due to its wide band gab, ZnO is transparent in the visible part of the electromagnetic spectrum. Highly n-doped ZnO:Al

 © 2007 Wiley-VCH Verlag GmbH & Co. KGaA, Weinheim

can therefore be used as a transparent conducting oxide (TCO).[93] The constituents Zn and Al are much cheaper and less poisonous compared to the generally used indium tin oxide (ITO). One application which has begun to be commercially available is the use of ZnO as the front contact for solar cells, which avoids the shadow effect necessarily associated with metal-finger contacts. Other appearing applications use ZnO as the front contact of liquid crystal displays[94] or ZnO:Al in the production of energy-saving or heat-protecting windows. A coating with TCO results in a glass which lets the visible part of the spectrum in but either reflects the IR back into the room (energy saving) or does not let the IR radiation into the room (heat protection), depending on which side of the window has the TCO coating.

12.2. Forthcoming Applications and Visions

Since the surface conductivity of ZnO can be strongly influenced by various gases, it is used as a gas sensor.[90,91]

The pointed tips of single crystals and nanorods (Figures 3 and 5) result in a strong enhancement of an electric field. Therefore, they can be used as field emitters.[92]

For the properties of ZnO as a UV-sensitive and solar-blind photodetector, see ref. [95] and for its hardness against high energy radiation, see ref. [96].

Furthermore, transparent thin-film transistors (TTFT) can be produced with ZnO. As field-effect transistors, they even may not need a p–n junction.[97] Some of the field-effect transistors even use ZnO nanorods as conducting channels.[98] An organic light-emitting diode (O-LED) has been described, which is transparent in the visible, deposited on a transparent plastic sheet and driven by a TTFT, the channel of which is based on ZnO.[99] Similarly, field-effect transistors (FET) with a channel consisting, for example, of a ZnO QW have been reported.[100] The vision is to use such transparent circuits on the front side of full-colour displays or on packaging material.

Now, we dwell for some time on various types of junctions. A rather simple one is a Schottky diode. The combination of n-type ZnO with Pd gives good rectifying contacts. In Figure 23, we show the current–voltage characteristics, plotting the log

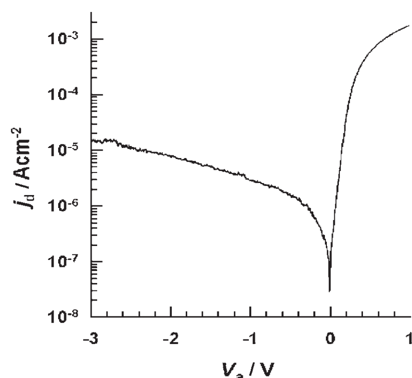

Figure 23. *I–V* characteristics of a ZnO/Pd Schottky diode, plotting the log of the modulus of the current as a function of the applied voltage.[101]

of the modulus of the current as a function of the applied voltage. One sees the exponential growth of the forward current until it bends over to a linear behaviour around 0.5 V and 10^{-3} A cm^{-2}, caused by the Ohmic resistance of ZnO. In blocking direction, the *I–V* characteristics show the (almost) constant saturation current of 10^{-5} A cm^{-2} below -1 V. The barrier height of the ZnO/Pd system is 1.1 eV.

For light-emitting diodes, there are reports on semiconductor homojunctions and heterojunctions. The idea of heterojunctions is to combine the easily available n-type ZnO with a good p-type semiconducting material, for example, n-ZnO/p-GaN or n-ZnO/p-SiC.[102] Though such systems are good as demonstrators, most of them will be of limited value concerning large-scale applications. If one already has a p-GaN layer, it will be most probably easier to continue with n-type GaN and not with ZnO. The combination with p-SiC has the disadvantage that SiC is an indirect-gap semiconductor with intrinsically low luminescence yield. Depending on the mobilities and the band alignment between n-ZnO and p-SiC, a certain fraction of the forward current in the heterojunction will be in the form of electrons travelling from the n-ZnO into the p-SiC and recombining there, mainly nonradiatively, while only the holes injected from p-SiC into n-ZnO will have a high probability of radiative recombination.

Recently, several groups reported on light-emitting diodes (LED) based on ZnO homojunctions,[103,104] partly with some $Zn_{1-x}Mg_xO$ barriers built in to influence carrier diffusion and recombination, an example of which is shown in Figure 24. This setup shows the typical *I–V* characteristics of a p–n junction and, in the forward direction, light emission. The spectrum consists of a tiny free-exciton emission band at 3.3 eV (see Figure 13 c), of a near-band emission peak in the blue and a rather broad band connected with deep-centre recombination (see Section 7). A similar broad band also appears in the photoluminescence spectrum of the p-type layer alone, showing that by far not all incorporated doping atoms in the p region form shallow acceptors, as ideally expected and discussed in Section 6.3. Consequently, it is useful to try at least pin junctions, in which the electron–hole-pair recombination occurs in a high-quality intrinsic layer. A further enhancement could come from the incorporation of one or several QWs in this intrinsic layer.[103,104] To the knowledge of the author, no reports exists to date concerning ZnO-based laser diodes.

To conclude this section on future applications, we present a vision concerning ferromagnetic ZnO:X (X = Mn, Co,Fe,...). If it becomes possible to create nanorods which are ferromagnetic at room temperature, and if it becomes possible to increase their magnetisation by several orders of magnitude (Section 8), and if it becomes possible to either flip the direction of magnetisation by an external field, for example, from a pixel on a magnetic data carrier and to read this process by the voltage induced in an nanocoil around the nanorod or vice–versa to control the magnetisation of the pixel by a current through the nanocoil, then the ZnO nanorods may be used as nano-sized read/write heads for magnetic data storage. The future must show whether or not there are too many "ifs"in the above sentence.

 © 2007 Wiley-VCH Verlag GmbH & Co. KGaA, Weinheim

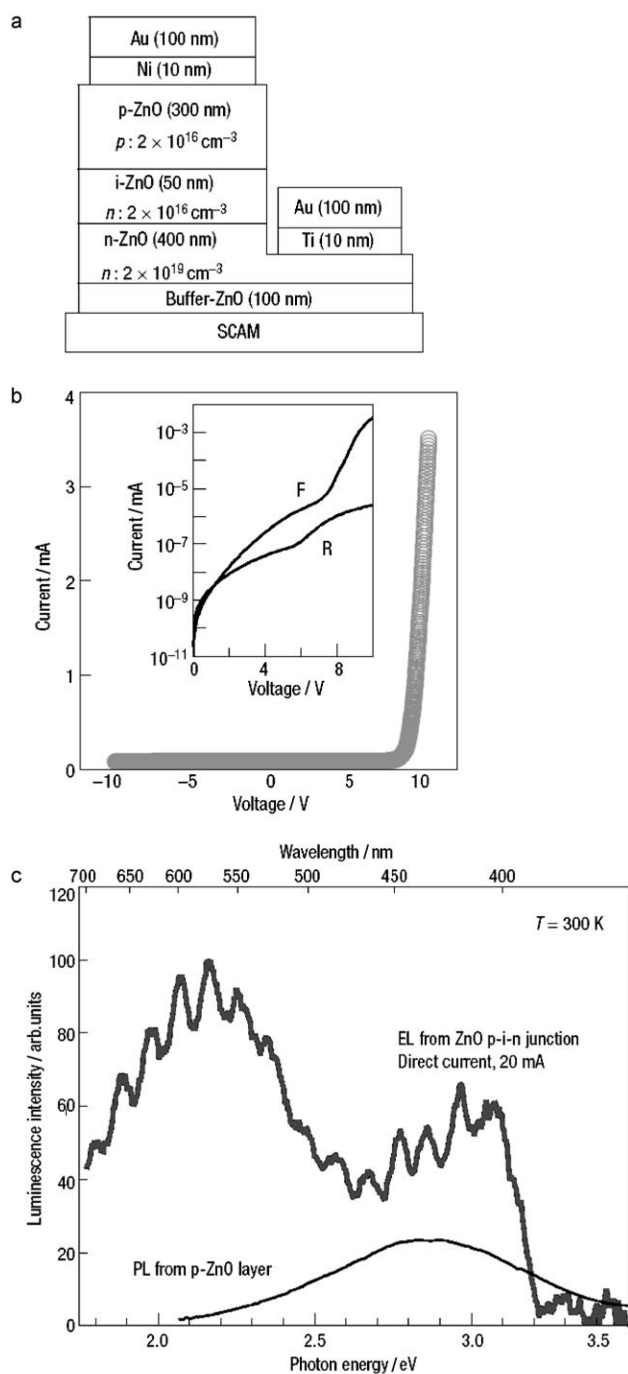

Figure 24. a) Setup, b) *I–V* characteristics (inset: logarithmic scale; F = forward bias, R = reverse bias) and c) electroluminescence (EL) and photoluminescence (PL) of a ZnO homojunction LED.[103]

13. Conclusion and Outlook

We took the reader on a tour d'horizon of various aspects of ZnO, starting from basic properties to real applications and visions of future uses. What we can say already is that beautiful physics can be performed with bulk ZnO and ZnO nanostructures. Whether it will be possible to master ZnO to a degree that allows wide applications in (transparent) electronics or optoelectronics is not yet clear. Since prophecy is a notoriously difficult task, nobody now can give a definite answer, but the perspectives are so exciting that it makes sense to invest ideas, money and work in this field during the next years.

Acknowledgements

The author would like to thank his Ph.D. supervisor Prof. Dr. E. Mollwo (†) of the Institut für Angewandte Physik of the University of Erlangen and the colleagues Prof. Dr. R. Helbig and Prof. Dr. K. Hümmer there for introducing him to ZnO research during his Diplom and Ph.D. theses. Actually, a lot of things were already common knowledge in the 1960s and 70s, as documented partly in the references below, at this institute and at some other places working on ZnO at that time, for example, in Berlin (Profs. Dr. I. Broser and A. Hoffmann) or Aachen (Prof. Dr. Heiland (†)), which are now being rediscovered by many young and eager scientists around the world. But also beautiful new physics is presently being discovered in ZnO by many groups around the world, which is also partly documented in the references. Concerning present activities, the author thanks his colleagues in Karlsruhe, Profs. Drs. H. Kalt and D. Gerthsen and their co-workers, as well as the co-workers in his own group (Drs. M. Schmidt, H. Priller, R. Hauschild, H. Zhou, and Dipl. Phys. J. Fallert to name only a few) for beautiful scientific work and for always stimulating discussions. Thanks for the latter aspects also goes to colleagues at other Universities, such as Profs. Drs. A. Waag (Braunschweig), B. Meyer (Giessen), A. Hoffmann (Berlin), R. Sauer, and K. Thonke (Stuttgart), M. Grundmann (Leipzig) T. Yao (Sendai), M. Willander (Göteborg) and J. M. Hvam (Odense, now Lyngby), again, to name just a few of the community. Financial support is acknowledged from the Landesstiftung Baden-Württemberg in project A1 of the Landeskompetenznetz "Funktionelle Nanostrukturen" and from the Deutsche Forschungsgemeinschaft.

Keywords: nanostructures · optical properties · oxides · semiconductors · zinc

Data collections like INSPEC or Web of Science give more than 18000 references for ZnO. Evidently, we can cite only a very limited selection, which cannot even include all relevant papers. Furthermore, it is not even possible to address individually all references below and their contents. Instead, we consider these references partly as "further reading" for those more deeply interested in the topic. We apologise for this shortcoming.

[1] P. H. Miller, Jr. in *Proc. Intern. Conf. on Semiconducting Materials Reading (1950)* (Ed.: H. K. Henisch), Butterworths, London, **1951**, p. 172.
[2] H. E. Brown, *Zinc Oxide Rediscovered*, The New Jersey Zinc Company, New York, **1957**; and *Zinc Oxide Properties and Applications*, Pergamon, New York, **1976**.
[3] H. Heiland, E. Mollwo, F. Stöckmann, *Solid State Phys.* **1959**, *8*, 191.
[4] W. Hirschwald with cooperation of P. Bonasewicz, L. Ernst, M. Grade. D. Hofmann, S. Krebs, R. Littbarski, G. Neumann, M. Grunze, D. Kolb, H. J. Schulz, *Curr. Top. Mater. Sci.* **1981**, *7*, 143.
[5] R. Helbig, Habilitation Thesis, Erlangen, **1975**.
[6] K. Hümmer, Habilitation Thesis, Erlangen, **1978**.
[7] C. Klingshirn, H. Haug, *Phys. Rep.* **1981**, *70*, 315.
[8] B. Hönerlage, R. Lévy, J. B. Grun, C. Klingshirn, K. Bohnert, *Phys. Rep.* **1985**, *124*, 161.
[9] *Landolt-Börnstein, New Series, Group III, Vol. 17 B, 22, 41 B* (Ed.: U. Rössler), Springer, Heidelberg, **1999**.

 © 2007 Wiley-VCH Verlag GmbH & Co. KGaA, Weinheim

[10] C. Klingshirn, *Semiconductor Optics, 3rd ed.*, Springer, Heidelberg, **2006**.
[11] "Zinc Oxide—A Material for Micro- and Optoelectronic Applications": *NATO Sci. Ser. 2* **2005**, *194*.
[12] C. Klingshirn, H. Priller, M. Decker, J. Brückner, H. Kalt, R. Hauschild, J. Zeller, A. Waag, A. Bakin, H. Wehmann, K. Thonke, R. Sauer, R. Kling, F. Reuss, Ch. Kirchner, *Adv. Solid State Phys.* **2005**, *45*, 261; C. Klingshirn, R. Hauschild, H. Priller, M. Decker, J. Zeller, H. Kalt, *Superlattices Microstruct.* **2005**, *38*, 209; C. Klingshirn, R. Hauschild, H. Priller, J. Zeller, M. Decker, H. Kalt, *NATO Sci. Ser. 2* **2006**, 231, 277.
[13] D. C. Look, B. Clafin, Ya. I. Alivov, S. J. Park, *Phys. Status Solidi A* **2004**, *201*, 2203.
[14] C. Klingshirn, M. Grundmann, A. Hoffmann, B. Meyer, A. Waag, *Phys. J.* **2006**, *5*, 33.
[15] Ü. Özgür, Ya. I. Avilov, C. Liu, A. Teke, M. A. Reshchikov, S. Dogan, V. Avrutin, S.-J. Cho, M. Morcoç, *J. Appl. Phys.* **2005**, *98*, 041301.
[16] *Zinc Oxide Bulk, Thin Films and Nanostructures*, (Eds.: C. Jagadish, S. J. Pearton), Elsevier, Amsterdam, **2006**.
[17] S. Desgreniers, *Phys. Rev. B* **1998**, *58*, 14102.
[18] R. W. Pohl, *Einführung in die Physik, Vol. 3, 10th ed.*, Springer, Heidelberg, **1958**.
[19] "Infrared Ellipsometry on Semiconductor Layer Structures: Phonons, Plasmons and Polaritons": M. Schubert, *Springer Tracts Mod. Phys.* **2004**, *209*.
[20] J. M. Calleja, M. Cardona, *Phys. Rev. B* **1977**, *16*, 3753.
[21] W. Glück, *Solid State Commun.* **1970**, *8*, 1831.
[22] E. Scharowski, *Z. Phys.* **1953**, *135*, 138; E. M. Dodson, J. A. Savage, *J. Mater. Sci.* **1968**, *3*, 19.
[23] R. Helbig, *J. Cryst. Growth* **1972**, *15*, 25.
[24] R. A. Laudise, A. A. Ballmann, *J. Phys. Chem.* **1960**, *64*, 688.
[25] E. Oshima, *J. Cryst. Growth* **2004**, *260*, 166.
[26] J. W. Nielsen, E. F. Dearborn, *J. Phys. Chem.* **1960**, *64*, 1762; J. Nause, B. Nemeth, *Semicond. Sci. Technol.* **2005**, *20*, S45; D. Schulz, S. Ganschow, D. Klimm, M. Neubert, M. Rossberg, M. Schmidbauer, R. Fornari, *J. Crystal Growth* **2006**, *296*, 27.
[27] *Landolt-Börnstein*, *New Series*, *Group III*, *Vol. 8*, **1972**.
[28] E. Mollwo, *Reichsber. Phys.* **1944**, *1*, 1.
[29] H. Schneck, R. Helbig, *Thin Solid Films* **1975**, *27*, 101.
[30] J. F. Muth, R. M. Kolbas, A. K. Sharma, S. Oktyabrsky, J. Naroyan, *J. Appl. Phys.* **1999**, *85*, 7884.
[31] Y. R. Ryu, S. Zhu, J. D. Budai, H. R. Chandrasekhar, P. F. Miceli, H. W. White, *J. Appl. Phys.* **2000**, *88*, 201; S. K. Hong, H. J. Ko, Y. Chen, T. Hanada, T. Yao, *J. Vac. Sci. Technol. B* **2000**, *18*, 2313; A. Zeuner, H. Alves, D. M. Hofmann, B. K. Meyer, *Appl. Phys. Lett.* **2002**, *80*, 2078; A. Uedono, T. Koida, A. Tsukazaki, M. Kawasaki, Z. Q. Chen, S. F. Chichibu, H. Koinuma, *J. Appl. Phys.* **2003**, *93*, 2481; Y. G. Wang, S. P. Lau, H. W. Lee, S. F. Yu, B. K. Tay, X. H. Zhang, H. H. Hng, *J. Appl. Phys.* **2003**, *94*, 354; Th. Gruber, C. Kirchner, R. Kling, F. Reuss, A. Waag, F. Bertram, D. Forster, J. Christen, M. Schreck, *Appl. Phys. Lett.* **2003**, *83*, 3290; A. Dadgar, N. Oleynik, D. Forster, S. Deiter, H. Witek, J. Bläsing, F. Bertram, A. Krtschil, A. Diez, J. Christen, A. Krost, *J. Cryst. Growth* **2004**, *267*, 140; Z. D. Sha, J. Wang, Z. C. Chen, A. J. Chen, Z. Y. Zhou, X. M. Wu, L. J. Zhuge, *Phys. E* **2006**, *33*, 263; Z. W. Liu, C. W. Sun, J. F. Gu, Q. Y. Zhang, *Appl. Phys. Lett.* **2006**, *88*, 251911.
[32] A. Ohtomo, M. Kawasaki, I. Ohkubo, H. Koinuma, T. Yasuda, Y Segawa, *Appl. Phys. Lett.* **1999**, *75*, 980; B. Bhattacharya, R. R. Das, R. S. Katiyar, *Appl. Phys. Lett.* **2003**, *83*, 2010; B. Bhattacharya, R. R. Das, R. S. Katiyar, *Thin Solid Films* **2004**, *447–448*, 564; Th. Gruber, C. Kirchner, R. Kling, F. Reuss, A. Waag, *Appl. Phys. Lett.* **2004**, *84*, 5359; M. Lorenz, H. Hochmuth, R. Schmidt-Grund, E. M. Kaisashev, M. Grundmann, *Ann. Phys.* **2004**, *13*, 59; C. Morhain, X. Tang, M. Teisseire-Doninelli, B. Lo, M. Laügt, J.-M. Chauveau, B. Vinter, O. Tottereau, P. Vennéguès, C. Deparis, G. Neu, *Superlattices Microstruct.* **2005**, *38*, 455; M. Lorenz, H. Hochmuth, J. Lenzner, G. Zimmermann, M. Diaconu, H. Schmidt, H. v. Wenchstern, M. Grundmann, *Thin Solid Films* **2005**, *486*, 205; P. Misra, T. K. Sharma, S. Porwal, L. M. Kukreja, *Appl. Phys. Lett.* **2006**, *89*, 161912; C. Sanjeeviraja, K. Ramamoorthy, M. Jayachandran, K. Sankaranarayanan, K. Misra, L. M. Kukrejy, *Curr. Appl. Phys.* **2006**, *6*, 103.
[33] Th. Passow, private communication, **2006**.
[34] Y.-S. Choi, C.-G. Lee, S. M. Cho, *Thin Solid Films* **1996**, *289*, 153; H. Zhou, D. M. Hofmann, A. Hofstätter, B. K. Meyer, *J. Appl. Phys.* **2003**, *94*, 1965; L. Castañeda, O. G. Morales-Saavedra, D. R. Acosta, A. Maldonado, M. de La Olvera, *Phys. Status Solidi A* **2006**, *203*, 1971.
[35] J. Y. Lao, J. Y. Huang, D. Z. Wang, Z. F. Ren, *Nano Lett.* **2003**, *3*, 235; J. Y. Lao, J. Y. Huang, D. Z. Wang, Z. F. Ren, *Nanowires and Nanobelts, Vols. 1 and 2* (Ed.: Z. L. Wang), Kluver, Boston, **2003**; R. Kling, A. Waag, *Nanotechnology* **2004**, *15*, 1043; T. Nobis, E. M. Kaidashev, A. Rahm, M. Lorenz, J. Lenzer, M. Grundmann, *Nano Lett.* **2004**, *4*, 797; T. Nobis, E. M. Kaidashev, A. Rahm, M. Lorenz, J. Lenzer, M. Grundmann, *Phys. Rev. Lett.* **2004**, *93*, 103903; Z. L. Wang, *J. Phys. Condens. Matter* **2004**, *16*, R829; G. C. Yi, C. Wang, W. I. Park, *Semicond. Sci. Technol.* **2005**, *20*, S22; G. C. Yi, C. Wang, W. I. Park, *Adv. Mater.* **2003**, *15*, 526; H. J. Fan, P. Werner, M. Zacharias, *Small* **2006**, *2*, 700; H. J. Fan, P. Werner, M. Zacharias, *Phys. J.* **2005**, *4*, 25; A. C. Mofor, A. S. Bakin, A. El-Shaer, D. Fuhrmann, F. Bertram, A. Hangleiter, J. Christen, A. Waag, *Phys. Status Solidi A* **2006**, *3*, 1046.
[36] M. Wissinger, H. Zhou, private communication, Karlsruhe, **2006**.
[37] M. Haupt, A. Ladenburger, R. Sauer, K. Thonke, R. Glass, W. Roos, J. P. Spatz, H. Rauscher, S. Riethmüller, M. Möller, *J. Appl. Phys.* **2003**, *93*, 6252.
[38] M. L. Fuller, *J. Appl. Phys.* **1944**, *15*, 164; A. B. Djurisic, Y. H. Leung, W. C. H. Choy, K. W. Cheah, W. K. Chan, *Appl. Phys. Lett.* **2004**, *84*, 2635.
[39] E. A. Meulenkamp, *J. Phys. Chem. B* **1998**, *102*, 5566; S. Mahamuni, K. Borgohain, B. S. Bendre, V. J. Leppert, S. H. Risbud, *J. Appl. Phys.* **1999**, *85*, 2861; E. M. Wong, P. C. Searson, *Appl. Phys. Lett.* **1999**, *74*, 2939; L. Guo, S. Yang, C. Yang, P. Yu, J. Wang, W. Ge, G. K. L. Wong, *Appl. Phys. Lett.* **2000**, *76*, 2901; Y. Harada, H. Kondo, N. Ichimura, S. Hashimoto, *J. Lumin.* **2000**, *87*, 405; H. Zhou, A. Alves, D. M. Hofmann, B. K. Meyer, G. Kaczmarczyk, A. Hoffmann, C. Thomsen, *Phys. Status Solidi B* **2002**, *229*, 825; A. P. A. Oliviera, J.-F. Hochepied, F. Grillon, M.-H. Berger, *Chem. Mater.* **2003**, *15*, 3202; S. Barik, A. K. Srivastave, P. Misra, R. V. Nandedkar, L. M. Kukreja, *Solid State Commun.* **2003**, *127*, 463; C. H. Kuhn, R. Lipski, F. Seeler, D. Mauder, G. Muller, L. Spanhel, *J. Sol-Gel Sci. Technol.* **2003**, *26*, 499; M. L. Kahn, M. Monge, V. Collière, F. Senocq, A. Maisonnat, B. Chaudret, *Adv. Funct. Mater.* **2005**, *15*, 458; W. Chen, G. Huang, H. Lu, D. E. McCready, A. G. Joly, J.-O. Bovin, *Nanotechnology* **2006**, *17*, 2595; J. G. Lu, Z. Z. Ye, Y. Z. Zhang, Q. L. Liang, Sz. Fujita, Z. L. Wang, *Appl. Phys. Lett.* **2006**, *89*, 023122.
[40] L. Mädler, W. J. Stark, S. E. Pratsinis, *J. Appl. Phys.* **2002**, *92*, 6537.
[41] D. C. Reynolds, C. W. Litton, T. C. Collins *Phys. Rev. A* **1965**, *140*, 1726.
[42] D. G. Thomas, *Phys. Chem. Solids* **1960**, *15*, 86; J. J. Hopfield, *Phys. Chem. Solids* **1960**, *15*, 97.
[43] M. Cardona, *J. Phys. Chem. Solids* **1963**, *24*, 1543; M. Cardona, *Phys. Rev.* **1963**, *129*, 69; K. Shindo, A. Morita, H. Kamimura, *J. Phys. Soc., Jap.* **1965**, *20*, 2054.
[44] A. V. Rodina, M. Strassburg, M. Dworzak, U. Haboeck, A. Hoffmann, A. Zeuner, H. R. Alves, D. M. Hofmann, B. K. Meyer, *Phys. Rev. B* **2004**, *69*, 125206; W. R. L. Lambrecht, A. V. Rodina, S. Limpijumnong, B. Segall, B. K. Meyer, *Phys. Rev. B* **2002**, *65*, 075207.
[45] A. R. Hutson, *Phys. Rev.* **1957**, *108*, 222; H. Rupprecht, *Phys. Chem. Solids* **1958**, *6*, 144; M. A. Seitz, D. H. Whitmore, *Phys. Chem. Solids* **1968**, *29*, 1033; C. Klingshirn, *Z. Phys.* **1971**, *248*, 433.
[46] P. Wagner, R. Helbig, *J. Phys. Chem. Solid* **1974**, *35*, 327.
[47] D. C. Look, D. C. Reynolds, J. R. Sizelove, R. L. Jones, C. W. Litton, G. Gantwell, W. C. Harsch, *Solid State Commun.* **1998**, *105*, 399.
[48] E. M. Kaidashew, M. Lorenz, H. v Wenckstern, A. Ralun, H.-C. Semmelhack, K.-H. Benndorf, C. Bundesmann, H. Hochmuth, M. Grundmann, *Appl. Phys. Lett.* **2003**, *82*, 3901; A. Ohtomo, A. Tsukazaki, *Semicond. Sci. Technol.* **2005**, *20*, S1; T. Makino, Y. Segawa, A. Tsukazaki, A. Ohtomo, M. Kawasaki, *Phys. Status Solidi C* **2006**, *3*, 956.
[49] K. Ellmer, *J. Phys. D* **2001**, *34*, 3097.
[50] W. I. Park, J. S. Kim, G.-C. Yi, M. H. Bae, H.-J. Lee, *Appl. Phys. Lett.* **2004**, *85*, 5052.
[51] Y. R. Ryu, T. S. Lee, H. W. White, *Appl. Phys. Lett.* **2003**, *83*, 87.
[52] E. Mosekilde, *Phys. Rev. B* **1970**, *2*, 3234; J. D. Albrecht, P. P. Ruden, S. Limpijumnong, W. R. L. Lambrecht, K. F. Brennan, *J. Appl. Phys.* **1999**, *86*, 6864; J. D. Albrecht, P. P. Ruden, S. Limpijumnong, W. R. L. Lambrecht, K. F. Brennan, *J. Appl. Phys.* **1999**, *86*, 6864.
[53] H. Tampo, H. Shibata, K. Matsubara, A. Yamada, P. Fons, S. Niki, M. Yamagata, H. Kanie, *Appl. Phys. Lett.* **2006**, *89*, 132113.
[54] A. Ohtomo, A. Tsukasaki, J. N. Njshii, H. Ohno, M. Kawasaki, 4th Intern. Workshop on ZnO and Rel. Mater., Giessen, Oct. 3–6, **2006**.

 © 2007 Wiley-VCH Verlag GmbH & Co. KGaA, Weinheim

[55] B. M. Ataev, A. M. Bagamadova, A. M. Djabrailov, V. V. Mamedov, R. A. Rabadanov, *Thin Solid Films* **1995**, *260*, 19; S. Y. Myong, S. J. Baik, C. H. Lee, W. Y. Cho, K. S. Lim, *Jpn. J. Appl. Phys.* **1997**, *36*, L1078; H. Kato, M. Sano, K. Miyamoto, T. Yao, *J. Cryst. Growth* **2002**, *237*–239, 538; T. Makino, Y. Segawa, S. Yoshida, A. Tsukazaki, A. Ohtomo, M. Kawasaki, *Appl. Phys. Lett.* **2004**, *85*, 759; T. Makino, Y. Segawa, S. Yoshida, A. Tsukazaki, A. Ohtomo, M. Kawasaki, H. Koinuma, *J. Appl. Phys.* **2005**, *98*, 093 520; S. W. Xue, X. T. Zu, W. G. Zheng, H. X. Deng, X. Xiang, *Phys. B* **2006**, *381*, 209.

[56] M. Göppert, F. Gehbauer, M. Hetterich, J. Münzel, D. Queck, C. Klingshirn, *J. Lumin.* **1997**, *72–74*, 430.

[57] B. Hahn, M. Worz, G. Meindel, E. Pschorr-Schoberer, W. Gebhardt, *Mater. Sci. Forum* **1998**, *287*–288, 339.

[58] M. Olvera, S. Tirado-Guerra, A. Maldonado, L. Castañeda, *Sol. Energy Mater. Sol. Cells* **2006**, *90*, 2346; C. G. Van de Walle, *Phys. Rev. Lett.* **2000**, *85*, 1012; D. M. Hofmann, A. Hofstaetter, F. Leiter, H. Zhou, F. Henecker, B. K. Meyer, S. Orlinskii, J. Schmidt, P. G. Baranov, *Phys. Rev. Lett.* **2002**, *88*, 045 504; M. D. McCluskey, S. J. Simpson, K. G. Lynn, *Appl. Phys. Lett.* **2002**, *81*, 3807; N. H. Nickel, K. Brendel, *Phys. Rev. B* **2003**, *68*, 193 303; Chr. van de Walle, J. Neugebauer, *Nature* **2003**, *423*, 626; Y. M. Strzhemechny, J. Nemergut, P. E. Smith, J. Bae, D. C. Look, L. J. Brillson, *J. Appl. Phys.* **2003**, *94*, 4256; G. A. Shi, M. Stavola, D. J. Pearton, M. Thieme, E. V. Lavrov, J. Weber, *Phys. Rev. B* **2005**, *72*, 195 211; E. V. Lavrov, F. Börnert, J. Weber, *Phys. Rev. B* **2005**, *72*, 085 212.

[59] J. J. Lander, *Phys. Chem. Solids* **1960**, *15*, 324; C. Klingshirn, E. Mollwo, *Z. Phys.* **1972**, *254*, 437; D. Zwingel, *J. Lumin.* **1972**, *5*, 385; D. Zwingel, F. Gärtner, *Solid State Commun.* **1974**, *14*, 45; S. V. Orlinskii, J. Schmidt, P. G. Baranov, D. M. Hofmann, *Phys. Rev. Lett.* **2004**, *92*, 047 603.

[60] K. Vanheusen, C. H. Seager, W. L. Warren, D. R. Tallant, J. A. Voigt, *Appl. Phys. Lett.* **1995**, *68*, 403; T. V. Butkhuzi, B. E. Tsekvava, N. P. Kekelidze, E. G. Chikoidze, T. G. Khulordava, M. M. Sharvahidze, *J. Phys. D* **1999**, *32*, 2683; E.-C. Lee, Y.-S. Kim, Y.-G. Jin, K. J. Chang, *Phys. Rev. B* **2001**, *64*, 085 120; S. B. Zhang, S.-H. Wei, A. Zunger, *Phys. Rev. B* **2001**, *63*, 075 205; X. L. Wu, G. G. Siu, C. L. Fu, H. C. Ong, *Appl. Phys. Lett.* **2001**, *78*, 2285; K. Nakahara, H. Takasu, P. Fons, A. Yamada, K. Iwata, K. Matsubara, R. Hunger, S. Niki, *J. Cryst. Growth* **2002**, *237–239*, 503; A. Zeuner, H. Alves, D. M. Hofmann, B. K. Meyer, A. Hoffmann, U. Haboeck, M. Strassburg, M. Dworzak, *Phys. Status Solidi B* **2002**, *234*, R7; T. Yamamoto, *Thin Solid Films* **2002**, *420–421*, 100; C. H. Park, S. B. Zhang, S.-H. Wei, *Phys. Rev. B* **2002**, *66*, 073 202; F. Leiter, H. Alves, D. Pfisterer, N. G. Romanov, D. M. Hofmann, B. K. Meyer, *Phys. B* **2003**, *340–342*, 201; K.-K. Kim, H.-S. Kim, D.-K. Hwang, J.-H. Lim, S.-J. Park, *Appl. Phys. Lett.* **2003**, *83*, 63; Y. R. Ryu, T. S. Lee, H. W. White, *Appl. Phys. Lett.* **2003**, *83*, 87; C. Zhang, X. Li, J. Bian, W. Yu, X. Gao, *Solid State Commun.* **2004**, *132*, 75; D. C. Look, B. Claflin, *Phys. Status Solidi B* **2004**, *241*, 624; Y. W. Heo, Y. W. Kwon, Y. Li, S. J. Pearton, D. P. Norton, *Appl. Phys. Lett.* **2004**, *84*, 3474; Y. W. Heo, K. Ip, S. J. Pearton, D. P. Norton, *Phys. Status Solidi A* **2004**, *201*, 1500; D. C. Look, G. M. Renlund, R. H. Burgener, J. R. Sizelove, *Appl. Phys. Lett.* **2004**, *85*, 5269; A. Krtschil, A. Dadgar, N. Oleynik, J. Bläsing, A. Diez, A. Krost, *Appl. Phys. Lett.* **2005**, *87*, 262 105; D. C. Look, *Semicond. Sci. Technol.* **2005**, ***20***, S55; A. Tsukazaki, A. Ohtomo, T. Onuma, M. Ohtani, T. Makino, M. Sumiya, K. Ohtani, S. F. Chichibu, S. Fuke, Y. Segawa, H. Ohno, H. Koinuma, M. Kawasaki, *Nat. Mater.* **2005**, *4*, 42; E. Kaminska, A. Piotrowska, J. Kossut, R. Butkute, W. Dobrowolski, R. Lukasiewicz, A. Barcz, R. Jakiela, E. Dynowska, E. Przezdziecka, M. Aleskiewicz, P. Wojnar, E. Kowalczyk, *Phys. Status Solidi C* **2005**, *2*, 1119; D. Pfisterer, J. Sann, D. M. Hofmann, B. Meyer, T. Frank, G. Pensl, R. Tena-Zaera, J. Zungiga-Pérez, C. Matinez-Tomas, V. Munoz-Sanjosé, *Phys. Status Solidi C* **2006**, *3*, 997; T. M. Borseth, B. G. Svensson, A. Y. Kuznetsov, P. Klason, Q. X. Zhao, M. Willander, *Appl. Phys. Lett.* **2006**, **89**, 262 112; B. Clafin, D. C. Look, S. J. Park, G. Cantwell, *J. Cryst. Growth* **2006**, *287*, 16; A. Krtschil, D. C. Look, Z-Q. Fang, A. Dadgar, A. Diez, A. Krost, *Phys. B* **2006**, *376–377*, 703; Y. Cao, L. Miao, S. Tanemura, M. Tanemura, Y. Kuno, Y. Hayashi, *Appl. Phys. Lett.* **2006**, *88*, 251 116.

[61] J. G. Lu, Y. Z. Zhang, Z. Z. Ye, L. P. Zhu, L. Wang, B. H. Zhao, Q. L. Liang, *Appl. Phys. Lett.* **2006**, *88*, 222 114; Y. J. Zeng, Z. Z. Ye, W. Z. Xu, D. Y. Li, G. J. Lu, L. P. Zhu, B. H. Zhao, *Appl. Phys. Lett.* **2006**, *88*, 062 107; J. Sann, A. Hofstaetter, D. Pfisterer, J. Stehr, B. K. Meyer, *Phys. Status Solidi C* **2006**, *4*, 952; Y. J. Zeng, Z. Z. Ye, W. Z. Xu, D. Y. Li, J. G. Lu, L. P. Zhu, B. H. Zhao, *Appl. Phys. Lett.* **2006**, *88*, 062 107.

[62] V. V. Osiko, *Opt. Spectrosc.* **1959**, *7*, 770; H. A. Weakliem, *J. Chem. Phys.* **1962**, *36*, 2117; R. E. Dietz, H. Kamimura, M. D. Sturge, A. Yariv, *Phys. Rev.* **1963**, *132*, 1559; Chr. Solbrig, *Z. Phys.* **1968**, *211*, 429; R. Dingle, *Phys. Rev. Lett.* **1969**, *23*, 579; F. W. Kleinlein, R. Helbig, *Z. Phys.* **1974**, *266*, 201; U. G. Kaufmann, P. Koidl, *J. Phys. C* **1974**, *7*, 791; G. Müller, *Phys. Status Solidi B* **1976**, *76*, 525; P. Koidl, *Phys. Rev. B* **1977**, *15*, 2493; F. G. Gärtner, E. Mollwo, *Phys. Status Solidi B* **1978**, *89*, 381; F. G. Gärtner, E. Mollwo, *Phys. Status Solidi B* **1978**, *90*, 33; R. Kuhnert, R. Helbig, *J. Lumin.* **1981**, *26*, 203; H.-J. Schulz, M. Thiede, *Phys. Rev. B* **1987**, *35*, 18; R. Heitz, A. Hofmann, I. Broser, *Phys. Rev. B* **1992**, *45*, 8977; K. Vanheusden, C. H. Seager, W. L. Warren, D. R. Tallant, J. A. Voigt, *Appl. Phys. Lett.* **1996**, *68*, 403; J. Xu, J. Zhang, W. Ding, W. Yang, Y. Du, J. Zuo, C. Xu, Y. Zhang, Z. Du, *Solid State Commun.* **1997**, *101*, 467; S. A. Studenikin, N. Golego, M. Cocivera, *J. Appl. Phys.* **1998**, *84*, 2287; X. L. Wu, G. G. Siu, C. L. Fu, H. C. Ong, *Appl. Phys. Lett.* **2001**, *78*, 2285; B. X. Lin, Z. X. Fu, Y. B. Jia, *Appl. Phys. Lett.* **2001**, *79*, 943; F. Leiter, H. Alves, D. Pfisterer, N. G. Romanov, D. M. Hofmann, B. K. Meyer, *Phys. B* **2003**, *340–342*, 201; D. Li, Y. H. Leung, A. B. Djurisic, Z. T. Liu, M. H. Xie, S. L. Shi, S. J. Xu, W. K. Chan, *Appl. Phys. Lett.* **2004**, *85*, 1601; E. Rita, U. Wahl, J. G. Correira, E. Alves, J. C. Soares, *Appl. Phys. Lett.* **2004**, *85*, 4899; X. Liu, X. Wu, H. Cao, R. P. H. Chang, *J. Appl. Phys.* **2004**, *95*, 3141; H. Priller, M. Decker, R. Hauschild, H. Kalt, C. Klingshirn, *Appl. Phys. Lett.* **2005**, *86*, 111 909; L. S. Vlasenko, G. D. Watkins, R. Helbig, *Phys. Rev. B* **2005**, *71*, 115 205; B. Kumar, H. Gonga, S. Vicknesh, S. J. Chua, S. Tripathy, *Appl. Phys. Lett.* **2006**, *89*, 141 901; L. Wu, Y. Wu, X. Pan, F. Kong, *Opt. Mater.* **2006**, *28*, 418; B. Cao, W. Cai, H. Zeng, *Appl. Phys. Lett.* **2006**, *88*, 161 101; D. Pfisterer, J. Sann, D. M. Hofmann, B. Meyer, Th. Frank, G. Pensl, R. Tena-Zaera, J. Zuñiga-Pérez, C. Martinez-Tomas, V. Muñoz-Sanjosé, *Phys. Status Solidi C* **2006**, *3*, 997; A. B. Djurisic, Y. H. Leung, K. H. Tam, L. Ding, W. K. Ge, H. Y. Chen, S. Gwo, *Appl. Phys. Lett.* **2006**, *88*, 103 107.

[63] D. Hahn, R. Nink, *Phys. Kondens. Mater.* **1965**, *3*, 311; D. Hahn, R. Nink, *Phys. Kondens. Mater.* **1966**, *4*, 336 ; B. Schallberger, A. Hausmann, *Z. Phys. B* **1981**, *44*, 143; A. F. Kohan, G. Ceder, D. Morgan, Chr. Van de Walle, *Phys. Rev. B* **2000**, *61*, 15 019; F. H. Leiter, H. R. Alves, A. Hofstaetter, D. M. Hofmann, B. K. Meyer, *Phys. Status Solidi B* **2001**, *226*, R4; Q. X. Zhao, P. Klason, M. Willander, H. M. Zhong, W. Lu, J. H. Yang, *Appl. Phys. Lett.* **2005**, *87*, 211 912.

[64] V. V. Osiko, *Opt. Spectrosc.* **1959**, ***7***, 770; H. A. Weakliem, *J. Chem. Phys.* **1962**, *36*, 2117; F. W. Kleinlein, R. Helbig, *Z. Phys.* **1974**, *266*, 201; U. G. Kaufmann, P. Koidl, *J. Phys. C* **1974**, *7*, 791; P. Koidl, *Phys. Rev. B* **1977**, *15*, 2493; F. G. Gärtner, E. Mollwo, *Phys. Status Solidi B* **1978**, *89*, 381; F. G. Gärtner, E. Mollwo, *Phys. Status Solidi B* **1978**, *90*, 33; H.-J. Schulz, M. Thiede, *Phys. Rev. B* **1987**, *35*, 18; R. Heitz, A. Hofmann, I. Broser, *Phys. Rev. B* **1992**, *45*, 8977; E. Rita, U. Wahl, J. G. Correira, E. Alves, J. C. Soares, *Appl. Phys. Lett.* **2004**, *85*, 4899; H. Priller, M. Decker, R. Hauschild, H. Kalt, C. Klingshirn, *Appl. Phys. Lett.* **2005**, *86*, 111 909.

[65] M. Hauser, Diplom Thesis, Karlsruhe, **2007**.

[66] A. C. Mofor, A. El-Shaer, A. Bakin, A. Waag, H. Ahlers, U. Siegner, S. Sievers, M. Albrecht, W. Schoch, N. Izyumskaya, V. Avrutin, S. Sorokin, S. Ivanov, J. Stoimenos, *Appl. Phys. Lett.* **2005**, *87*, 62 501.

[67] T. Dietl, H. Ohno, F. Matsukura, J. Cibert, D. Ferrand, *Science* **2000**, *287*, 1019; K. Ueda, H. Tabata, T. Kawai, *Appl. Phys. Lett.* **2001**, *79*, 988; K. Sato, H. Katayama-Yoshida, *Semicond. Sci. Technol.* **2002**, *17*, 367; H. Zhou, D. M. Hofmann, A. Hofstaetter, B. K. Meyer, *J. Appl. Phys.* **2003**, *94*, 1965; D. A. Schwartz, N. S. Norberg, Q. P. Nguyen, J. M. Parker, D. R. Gamelin, *J. Am. Chem. Soc.* **2003**, *125*, 13 205; P. Sharma, A. Gupta, K. V. Rao, F. J. Owens, R. Sharma, R. Ahuja, J. M. O. Guillen, B. Johansson, G. A. Gehring, *Nat. Mater.* **2003**, *2*, 673; N. Jedrecy, H. J. v. Bardeleben, Y. Zheng, J.-L. Cantin, *Phys. Rev. B* **2004**, *69*, 041 308(R); S. J. Pearton, W. H. Heo, D. P. Norton, T. Steiner, *Semicond. Sci. Technol.* **2004**, *19*, R59; A. C. Mofor, E. El-Shaer, A. Bakin, A. Waag, H. Ahlers, U. Siegner, M. Albrecht, W. Schoch, N. Izyunkskaya, V. Avrutin, S. Sorokin, S. Ivanov, J. Stoimenos, *Appl. Phys. Lett.* **2005**, *87*, 62 501; A. C. Mofor, E. El-Shaer, A. Bakin, A. Waag, H. Ahlers, U. Siegner, M. Albrecht, W. Schoch, N. Izyunkskaya, V. Avrutin, S. Sorokin, S. Ivanov, J. Stoimenos, *Phys. Status Solidi C* **2006**, *4*, 1104; C. Liu, F. Yun, M. Morkoç, *J. Mater. Sci.* **2005**, *40*, 555; H.-J. Lee, S. H. Choi, C. R. Cho, H. K. Kim, S.-Y. Jeong, *Europhys. Lett.* **2005**, *72*, 76; K. Ando, *Science* **2006**, *312*, 1883; S. Yin, M. X. Xu, L. Yang, J. F. Liu, H. Rösner, H. Hahn, H. Gleiter, D. Schild, S. Doyle, T. Liu, T. D. Hu, E. Takayama-Muromachi, J. Z. Jiang, *Phys. Rev. B*

 © 2007 Wiley-VCH Verlag GmbH & Co. KGaA, Weinheim

2006, *73*, 224408; U. Philipose, S. V. Nair, S. Trudel, R. H. Hill, H. E. Ruda, *Appl. Phys. Lett.* **2006**, *88*, 263101; O. D. Jayakumar, I. K. Gopalakrishnan, S. K. Kulshrestha, *Phys. B* **2006**, *381*, 194; M. Abid, J.-P. Abid, J.-Ph. Ansermet, *J. Electrochem. Soc.* **2006**, *153*, D138; J. B. Wang, G. J. Huang, X. L. Zhong, L. Z. Sun, Y. C. Zhou, E. H. Liu, *Appl. Phys. Lett.* **2006**, *88*, 252502; N. Khare, M. J. Kappers, M. Wei, M. G. Blamire, J. L. MacManus-Driscoll, *Adv. Mater.* **2006**, *18*, 1449; J. Blasco, F. Bartolomé, L. M. Garcia, J. Garcia, *J. Mater. Chem.* **2006**, *16*, 2282; L. Q. Liu, B. Xiang, X. Z. Zhang, D. P. Yu, *Appl. Phys. Lett.* **2006**, *88*, 063104; H. Zhou, C. Knies, D. M. Hofmann, J. Stehr, N. Volbers, B. K. Meyer, L. Chen, P. Klar, W. Heimbrodt, *Phys. Status Solidi A* **2006**, *203*, 2756; H. S. Hsu, J. C. Huang, Y. H. Huang, Y. F. Liao, M. Z. Lin, C. H. Lee, J. F. Lee, S. F. Chen, L. Y. Lai, C. P. Liu, *Appl. Phys. Lett.* **2006**, *88*, 242507; A. Hernado, A. Quesada, M. A. Garcia, P. Crespo, *J. Magn. Magn. Mater.* **2006**, *304*, 75; J. Wang, Z. Gu, M. Lu, D. W. Wu, C. Yuan, S. Zhang, Y. Chen, S. Zhu, Y. Zhu, *Appl. Phys. Lett.* **2006**, *88*, 252110; W. B. Jian, Z. Y. Wu, R. T. Huang, F. R. Chen, J. J. Kai, C. Y. Wu, S. J. Chiang, M. D. Lan, J. J. Lin, *Phys. Rev. B* **2006**, *73*, 233308; H. Zhou, Ch. Knies, D. M. Hofmann, J. Stehr, N. Valhers, B. K. Meyer, L. Chen, P. Klar, W. Heimbrodt, *Phys. Stat. Sol.* **2006**, *203*, 2756; H. J. Lee, S. H. Choi, C. R. Cho, H. K. Kim, S. Y. Jeong, *Europhys. Lett.* **2005**, *72*, 76.

[68] R. Hauschild, H. Priller, M. Decker, J. Brückner, H. Kalt, C. Klingshirn, *Phys. Status Solidi C* **2006**, *3*, 976.

[69] E. Tomzig, R. Helbig, *J. Lumin.* **1976**, *14*, 403; G. Blattner, C. Klingshirn, R. Helbig, R. Meinl, *Phys. Status Solidi B* **1981**, *107*, 105; R. Thonke, K. Sauer, *Springer Ser. Solid-State Phys.* **2004**, *146*, 73; B. K. Meyer, H. Alves, D. M. Hofmann, W. Kriegseis, T. Riemann, J. Christen, A. Hoffmann, M. Strassburg, M. Dvorzak, U. Haboeck, A. V. Rodina, *Phys. Status Solidi B* **2004**, *241*, 231.

[70] J. H. Hvam, *Sol. State Commun.* **1973**, *12*, 95.

[71] C. Klingshirn, *Phys. Status Solidi B* **1975**, *71*, 547.

[72] Priller, J. Brückner, Th. Gruber, C. Klingshirn, H. Kalt, A. Waag, H. J. Ko, T. Yao, Intern. II–VI Conf. in Buffalo, New York, Niagara Falls, 22–26 Sept. 2003; Priller, J. Brückner, Th. Gruber, C. Klingshirn, H. Kalt, A. Waag, H. J. Ko, T. Yao, *Phys. Status Solidi B* **2004**, *241*, 587.

[73] J. M. Hvam, G. Blattner, M. Reuscher, C. Klingshirn, *Phys. Status Solidi B* **1983**, *118*, 179.

[74] J. Fallert, R. Hauschild, A. Urban, H. Priller, H.Kalt, C. Klingshirn, *Proc. 28th ICPS*, Wien (**2006**) in press (**2007**); C. Klingshirn, R. Hauschild, F. Fallert, H. Kalt, *Phys. Rev. B* **2007**, *75*, 115203.

[75] R. Zimmermann, *Many Particle Theory of Highly Excited Semiconductors, Teubner Texte Phys.*, Teubner, Leipzig, **1988**.

[76] C. Klingshirn, *Solid State Commun.* **1973**, *13*, 297; W. Wünstel, C. Klingshirn, *Opt. Commun.* **1980**, *32*, 269.

[77] F. H. Nicoll, *Appl. Phys. Lett.* **1966**, *9*, 13; J. R. Packard, D. A. Campbell, W. C. Tait, *J. Appl. Phys.* **1967**, *38*, 5255; F. H. Nicoll, *J. Appl. Phys.* **1968**, *39*, 4469; S. Iwai, S. Namba, *Appl. Phys. Lett.* **1970**, *16*, 354; J. R. Packard, W. C. Tait, G. H. Dierssen, *Appl. Phys. Lett.* **1971**, *19*, 338; T. Goto, D. W. Langer, *J. Appl. Phys.* **1971**, *42*, 5066; W. D. Johnson, *J. Appl. Phys.* **1971**, *42*, 2731; J. Shewchun, B. K. Garside, B. S. Kawasaki, T. Efthymiopoulos, *J. Appl. Phys.* **1972**, *43*, 545; B. Hönerlage, C. Klingshirn, J. B. Grun, *Phys. Status Solidi B* **1976**, *78*, 599; S. W. Koch, H. Haug, G. Schmieder, W. Bohnert, C. Klingshirn, *Phys. Status Solidi B* **1978**, *89*, 431.

[78] K. Bohnert, G. Schmieder, C. Klingshirn, *Phys. Status Solidi B* **1980**, *98*, 175; K. Bohnert, M. Anselment, G. Kobbe, C. Klingshirn, H. Haug, S. W. Koch, S. Schmitt-Rink, F. F. Abraham, *Z. Phys. B* **1981**, *42*, 1.

[79] D. M. Bagnall, Y. F. Chen, Z. Zhu, T. Yao, S. Koyama, M. Y. Shen, T. Goto, *Appl. Phys. Lett.* **1997**, *70*, 2230.

[80] D. M. Bagnall, Y. F. Chen, Z. Zhu, T. Yao, M. Y. Shen, T. Goto, *Appl. Phys. Lett.* **1998**, *73*, 1038.

[81] Y. Chen, N. T. Tuan, Y. Segawa, H. Ko, S. Hong, T. Yao, *Appl. Phys. Lett.* **2001**, *78*, 1469.

[82] S. Cho, J. Ma, Y. Kim, Y. Sun, G. K. L. Wong, J. B. Ketterson, *Appl. Phys. Lett.* **1999**, *75*, 2761.

[83] P. Yu, Z. K. Wang, G. K. Wong, M. Kawasaki, A. Ohtomo, H. Koinuma, Y. Segawa, *J. Cryst. Growth* **1998**, *184*, 601; C. Klingshirn, M. Grundmann, A. Hoffmann, B. K. Meyer, A. Waag, *Phys. J.* **2006**, *5*, 33.

[84] P. Yu, Z. K. Tang, G. K. L. Wong, M. Kawasaki, A. Ohtomo, H. Koinuma, Y. Segawa, *Proceedings of 23th ICPS-World Scientific,* Singapore, *2*, 1453, **1996**.

[85] H. D. Sun, T. Makino, N. T. Tuan, Y. Segawa, Z. T. Tang, G. K. L. Wong, M. Kawasaki, A. Ohtomo, K. Tamura, H. Koinuma, *Appl. Phys. Lett.* **2000**, *77*, 4250.

[86] M. H. Huang, S. Mao, H. Feick, H. Yan, Y. Wu, H. Kind, E. Weber, R. Russo, P. Yang, *Science* **2001**, *292*, 1897; J. C. Johnson, H. Yan, P. Yang, R. J. Saykally, *J. Phys. Chem. B* **2003**, *107*, 8816; Z. Qiu, K. S. Wong, M. Wu, W. Lin, H. Xu, *Appl. Phys. Lett.* **2004**, *84*, 2739; Y. H. Leung, W. M. Kwok, A. B. Djurisic, D. L. Phillips, W. K. Chan, *Nanotechnology* **2005**, *16*, 579; Y. Zhang, R. E. Russo, S. S. Mao, *Appl. Phys. Lett.* **2005**, *87*, 043106; B. Zou, R. Liu, F. Wang, A. Pan, L. Cao, Z. L. Wang, *J. Phys. Chem. B* **2006**, *110*, 12865.

[87] T. Nobis, E. M. Kaidashev, A. Rahm, M. Lorenz, M. Grundmann, *Phys. Rev. Lett.* **2004**, *93*, 103903.

[88] R. Hauschild, H. Lange, H. Priller, C. Klingshirn, R. Kling, A. Waag, H. J. Fan, M. Zacharias, H. Kalt, *Phys. Status Solidi B* **2006**, *243*, 853; R. Hauschild, H. Kalt, *Appl. Phys. Lett.* **2006**, *89*, 123107.

[89] H. Cao, Y. G. Zhao, H. C. Ong, S. T. Ho, J. Y. Dai, J. Y. Wu, R. P. H. Chang, *Appl. Phys. Lett.* **1998**, *73*, 3656; R. K. Thareja, A. Mitra, *Appl. Phys. B* **2000**, *71*, 181; H. Cao, Y. Ling, J. Y. Xu, C. Q. Cao, P. Kumar, *Phys. Rev. Lett.* **2001**, *86*, 4524; H. C. Junying, Y. Xu, Y. Ling, A. L. Burin, E. W. Seeling, X. Liu, R. P. H. Chang, *IEEE J. Sel. Top. Quantum Electron.* **2003**, *9*, 111; D. Anglos, A. Stassinopoulos, R. N. Das, G. Zacharakis, M. Psyllaki, R. Jakubiak, R. A. Vaia, E. P. Giannelis, S. H. Anastasiadis, *J. Opt. Soc. Am. B* **2004**, *21*, 208; S. F. Yu, C. Yuen, S. P. Lau, W. I. Park, G.-C. Yi, *Appl. Phys. Lett.* **2004**, *84*, 3241; V. M. Markushev, M. V. Ryzhkov, Ch. M. Briskina, H. Cao, *Laser Phys.* **2005**, *15*, 1611; A. C. Vutha, S. K. Tiwari, R. K. Thareja, *J. Appl. Phys.* **2006**, *99*, 123509; V. M. Markushev, M. V. Ryzhkokv, C. M. Briskina, *Appl. Phys. B* **2006**, *84*, 333.

[90] G. Heiland, *Z. Phys.* **1954**, *138*, 459; E. Mollwo, *Z. Phys.* **1954**, *138*, 478; G. Heiland, *Z. Phys.* **1955**, *142*, 415; G. Heiland, *Z. Phys.* **1957**, *148*, 15.

[91] E. Comini, G. Faglia, G. Sberveglieri, Z. Pan, Z. L. Wang, *Appl. Phys. Lett.* **2002**, *81*, 1869; N. Kumar, A. Dorfmann, J.-i. Hahm, *Nanotechnology* **2006**, *17*, 2875; J. Suehiro, N. Nakagawa, S.-i. Hidaka, M. Ueda, K. Imasa, M. Higashihata, T. Okada, M. Hara, *Nanotechnology* **2006**, *17*, 2567.

[92] K. P. Frohmader, *Solid State Commun.* **1969**, *7*, 1543; Q. Wan, K. Yu, T. H. Wang, C. L. Lin, *Appl. Phys. Lett.* **2003**, *83*, 2253; Y. B. Li, Y. Bando, D. Golberg, *Appl. Phys. Lett.* **2004**, *84*, 3603; Q. H. Li, Q. Wan, Y. J. Chen, T. H. Wang, H. B. Jia, D. P. Yu, *Appl. Phys. Lett.* **2004**, *85*, 636; F. Xu, G. Li, Q. Li, Z. Zhu, *Nanotechnology* **2006**, *17*, 2855; N. S. Ramgir, D. J. Late, A. B. Bhise, I. S. Mulla, M. A. More, D. S. Joag, V. K. Pillai, *Nanotechnology* **2006**, *17*, 2730; Y. Zhang, K. Yu, S. Ouyang, Z. Zhu, *Phys. B* **2006**, *382*, 76.

[93] T. Minami, H. Nanot, S. Takata, *Jpn. J. Appl. Phys.* **1984**, *23*, L280; P. Kuppusami, K. Diesner, I. Sieber, K. Ellmer, *Mater. Res. Soc. Symp. Proc.* **2002**, *721*, 171; C. Agashe, O. Kluth, G. Schope, H. Siekmann, J. Hupkes, B. Rech, *Thin Solid Films* **2002**, *442*, 167.

[94] B.-Y. Oh, M.-C. Jeong, T.-H. Moon, W. Lee, J.-M. Myoung, J.-Y. Hwang, D.-S. Seo, *J. Appl. Phys.* **2006**, ***99***, 124505.

[95] E. Mollwo, *Z. Phys. Chem.* **1951**, *198*, 257; H. Weiss, *Z. Phys.* **1952**, *132*, 335; G. Heiland, *Phys. Chem. Solids* **1958**, *6*, 155; P. Sharma, A. Mansingh, K. Sreenivas, *Appl. Phys. Lett.* **2002**, *80*, 553; Y. R. Ryu, T. S. Lee, J. A. Lubguban, H. W. White, Y. S. Park, C. J. Youn, *Appl. Phys. Lett.* **2005**, *87*, 153504.

[96] J. F. Cordaro, C. E. Shipway, J. T. Schott, *J. Appl. Phys.* **1987**, *61*, 429; D. C. Look, D. C. Reynolds, J. W. Hemsky, R. L. Jones, J. R. Sizelove, *Appl. Phys. Lett.* **1999**, *75*, 811; C. Coskun, D. C. Look, G. C. Farlow, J. R. Sizelove, *Semicond. Sci. Technol.* **2004**, *19*, 752; F. Tuomisto, K. Saarinen, D. C. Look, *Phys. Status Solidi A* **2004**, *201*, 2219.

[97] K. Nomura, H. Ohta, K. Ueda, T. Kamiya, M. Hirano, H. Hosono, *Science* **2003**, *300*, 1269; S. Masuda, K. Kitamura, Y. Okumura, S. Miyatake, H. Tabata, T. Kawai, *J. Appl. Phys.* **2003**, *93*, 1624; R. L. Hoffman, B. J. Norris, J. F. Wager, *Appl. Phys. Lett.* **2003**, *82*, 733; R. L. Hoffman, *J. Appl. Phys.* **2004**, *95*, 5813; Y. J. Li, Y. W. Kwon, M. Jones, Y. W. Heo, J. Zhou, S. C. Luo, P. H. Holloway, E. Douglas, D. P. Norton, Z. Park, S. Li, *Semicond. Sci. Technol.* **2005**, *20*, 720; J. Nishii, A. Ohtomo, K. Ohtani, H. Ohno, M. Kawasaki, *Jpn. J. Appl. Phys.* **2005**, *44*, L1195; A. Ohtomo, S. Takagi, K. Tamura, T. Makino, Y. Segawa, H. Koinuma, M. Kawasaki, *Jpn. J. Appl. Phys.* **2006**, *45*, L694.

[98] Y. W. Heo, L. C. Tien, Y. Kwon, D. P. Norton, S. J. Pearton, B. S. Kang, F. Ren, *Appl. Phys. Lett.* **2004**, *85*, 2274; W. I. Park, J. S. Kim, G.-C. Yi, M. H.

 © 2007 Wiley-VCH Verlag GmbH & Co. KGaA, Weinheim

Bae, H.-J. Lee, *Appl. Phys. Lett.* **2004**, *85*, 5052; Z. Fan, D. Wang, P.-C. Chang, W.-Y. Tseng, J. G. Lu, *Appl. Phys. Lett.* **2004**, *85*, 5923; Z. Fan, D. Wang, P.-C. Chang, W.-Y. Tseng, J. G. Lu, *Appl. Phys. Lett.* **2004**, *85*, 5923; R. L. Hoffman, B. J. Norris, J. F. Wager, *Appl. Phys. Lett.* **2003**, *82*, 733; W. I. Park, J. S. Kim, G.-C. Yi, H.-J. Lee, *Adv. Mater.* **2005**, *17*, 1393; H.-J. Kim, C.-H. Lee, D.-W. Kim, G.-C. Yi, *Nanotechnology* **2006**, *17*, S327.

[99] P. Gorrn, T. Rabe, W. Kowalsky, F. Galbrecht, U. Scherf, *Appl. Phys. Lett.* **2006**, *89*, 161113 and contributions RI-03 and RIX-03 to E-MRS meeting, Nice, **2006**.

[100] K. Koike, I. Nakashima, K. Hashimoto, S. Sasa, M. Inoue, M. Yano, *Appl. Phys. Lett.* **2005**, *87*, 112106.

[101] M. Grundmann, H. v. Wenckstern, R. Pickenhain, T. Nobis, A. Rahm, M. Lorenz, *Superlattices Microstruct.* **2005**, *38*, 317.

[102] Y. I. Alivov, J. E. van Nostrand, D. C. Look, M. V. Chukichev, B. M. Ataev, *Appl. Phys. Lett.* **2003**, *83*, 2943; Q.-X. Yu, B. Xu, Q.-H. Wu, Y. Liao, G.-Z. Wang, R.-C. Fang, H.-Y. Lee, C.-T. Lee, *Appl. Phys. Lett.* **2003**, *83*, 4713; Y. I. Alivov, E. V. Kalinina, A. E. Cherenkkov, D. C. Look, B. M. Ataev, A. K. Omaev, M. V. Chukichev, D. M. Bagnall, *Appl. Phys. Lett.* **2003**, *83*, 4719; W. I. Park, G.-C. Yi, *Adv. Mater.* **2004**, *16*, 87; S. F. Chichibu, T. Ohomori, N. Shibata, T. Koyama, T. Onuma, *Appl. Phys. Lett.* **2004**, *85*, 4403; A. Osinsky, J. W. Dong, M. Z. Kauser, B. Hertog, A. M. Dabiran, P. P. Chow, S. J. Pearton, O. Lopatiuk, L. Chernyak, *Appl. Phys. Lett.* **2004**, *85*, 4272; R. Könenkamp, R. C. Word, C. Schlegel, *Appl. Phys. Lett.* **2004**, *85*, 6004; H. S. Yang, S. Y. Han, Y. W. Heo, K. H. Baik, D. P. Norton, S. J. Pearton, F. Ren, A. Osinsky, J. W. Dong, B. Hertog, A. M. Dabiran, P. P. Chow, L. Chernyak, T. Steiner, C. J. Kao, G. C. Chi, *Jpn. J. Appl. Phys.* **2005**, *44*, 7296; H. Sun, Q.-F. Zhang, J.-L. Wu, *Nanotechnology* **2006**, *17*, 2271; A. V. Osinsky, J. W. Dong, J. Q. Xie, B. Hertog, A. M. Dabiran, P. P. Chow, S. J. Pearton, D. P. Norton, D. C. Look, W. Schoenfeld, O. Lopatiuk, L. Chernyak, M. Cheung, A. N. Cartwright, M. Gerhold, *Mater. Res. Soc. Symp. Proc.* **2006**, *892*, 429; S. J. Jiao, Y. M. Lu, D. Z. Shen, Z. Z. Zhang, B. H. Li, J. Y. Zhang, B. Yao, Y. C. Liu, X. W. Fan, *Phys. Status Solidi C* **2006**, *4*, 972; C. Peiliang, M. Xiangyang, Y. Deren, *Appl. Phys. Lett.* **2006**, *89*, 111112.

[103] A. Tsukazaki, A. Ohtomo, T. Onuma, M. Ohtani, T. Makino, M. Sumiya, K. Ohtani, S. F. Chichibu, S. Fuke, Y. Segawa, H. Ohno, H. Koinuma, M. Kawasaki, *Nat. Mater.* **2005**, *4*, 42.

[104] A. Tsukazaki, M. Kubota, A. Ohtomo, T. Onuma, K. Ohtani, H. Ohno, S. F. Chichibu, M. Kawasaki, *Jpn. J. Appl. Phys.* **2005**, *44*, L643; Y. Ryu, T.-S. Lee, J. A. Lubguban, H. W. White, B.-J. Kim, Y.-S. Park, C.-J. Youn, *Appl. Phys. Lett.* **2006**, *88*, 241108; S. J. Jiao, Z. Z. Zhang, Y. M. Lu, D. Z. Shen, B. Yao, J. Y. Zhang, B. H. Li, D. X. Zhao, X. W. Fan, Z. K. Tang, *Appl. Phys. Lett.* **2006**, *88*, 031911; H. White, Y. Ryu, *Opto Laser Europe* **2006**, *143*, 26.

Received: January 2, 2007

 © 2007 Wiley-VCH Verlag GmbH & Co. KGaA, Weinheim